

# Introduction to The Theory of Superconductivity

Cryocourse 2009  
Helsinki, Finland

N. B. Kopnin  
Low Temperature Laboratory,  
Helsinki University of Technology,  
P.O. Box 2200, FIN-02015 HUT, Finland

September 7, 2009



# Contents

<b>1</b>	<b>Introduction</b>	<b>5</b>
1.1	Superconducting transition . . . . .	5
1.2	The London model . . . . .	7
1.2.1	Meissner effect . . . . .	8
1.3	Phase coherence . . . . .	9
1.3.1	Magnetic flux quantization . . . . .	9
1.3.2	Coherence length and the energy gap . . . . .	10
1.4	Critical currents and magnetic fields . . . . .	11
1.4.1	Condensation energy . . . . .	11
1.4.2	Critical currents . . . . .	12
1.5	Quantized vortices . . . . .	13
1.5.1	Basic concepts . . . . .	13
1.5.2	Vortices in the London model . . . . .	15
1.5.3	Critical fields in type-II superconductors . . . . .	16
<b>2</b>	<b>The BCS theory</b>	<b>19</b>
2.1	Landau Fermi-liquid . . . . .	19
2.2	The Cooper problem . . . . .	22
2.3	The BCS model . . . . .	26
2.3.1	The Bogoliubov–de Gennes equations . . . . .	26
2.3.2	The self-consistency equation . . . . .	26
2.4	Observables . . . . .	26
2.4.1	Energy spectrum and coherence factors . . . . .	26
2.4.2	Density of states . . . . .	28
2.4.3	The energy gap . . . . .	29
2.4.4	Current . . . . .	31
<b>3</b>	<b>Andreev reflection</b>	<b>33</b>
<b>4</b>	<b>Weak links</b>	<b>39</b>
4.1	Josephson effect . . . . .	39
4.1.1	D.C and A.C. Josephson effects . . . . .	39
4.1.2	Superconducting Quantum Interference Devices . . . . .	42
4.2	Dynamics of Josephson junctions . . . . .	42

4.2.1	Resistively shunted Josephson junction . . . . .	42
4.2.2	The role of capacitance . . . . .	44
4.2.3	Thermal fluctuations . . . . .	49
4.2.4	Shapiro steps . . . . .	51
<b>5</b>	<b>Coulomb blockade in normal double junctions</b>	<b>53</b>
5.1	Orthodox description of the Coulomb blockade . . . . .	53
5.1.1	Low temperature limit . . . . .	56
5.1.2	Conductance in the high temperature limit . . . . .	57
<b>6</b>	<b>Quantum phenomena in Josephson junctions</b>	<b>59</b>
6.1	Quantization . . . . .	59
6.1.1	Quantum conditions . . . . .	59
6.1.2	Charge operator . . . . .	60
6.1.3	The Hamiltonian . . . . .	62
6.2	Macroscopic quantum tunnelling . . . . .	63
6.2.1	Effects of dissipation on MQT . . . . .	65
6.3	Band structure . . . . .	66
6.3.1	Bloch's theorem . . . . .	66
6.3.2	Bloch's theorem in Josephson devices . . . . .	67
6.3.3	Large Coulomb energy: Free-phase limit . . . . .	68
6.3.4	Low Coulomb energy: Tight binding limit . . . . .	70
6.4	Coulomb blockade . . . . .	71
6.4.1	Equation of motion . . . . .	72
6.4.2	Bloch oscillations and the Coulomb blockade in Josephson junctions . . . . .	72
6.4.3	Effect of dissipation . . . . .	75
6.5	Parity effects . . . . .	76

# Chapter 1

## Introduction

### 1.1 Superconducting transition

Superconductivity manifests itself mainly as an absence of resistivity below some critical temperature. It was discovered in 1911 by H. Kamerlingh Onnes in Leiden, three years after he first liquefied  $^4\text{He}$ . He measured the resistivity of mercury. The resistivity behavior as a function of temperature is shown in Fig. 1.1.

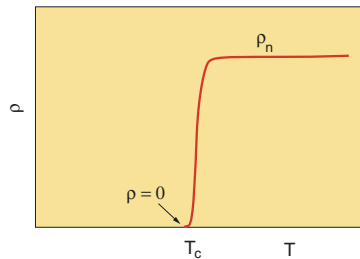


Figure 1.1: Below the transition temperature, the resistivity drops to zero.

The absolute absence of resistivity is a very fundamental phenomenon. In combination with general quantum-mechanical principles, it can lead to quite informative conclusions on the properties of the superconducting state. Here we try to describe the basic picture of superconductivity using minimum amount of input information. We consider the most striking properties of superconductors such as their ideal diamagnetism, macroscopic quantum nature of superconductivity including phase coherence which leads to zero resistivity, to quantization of magnetic flux and to formation of quantized vortices. The maximum values of magnetic fields and currents that can be withstood by superconductors are also briefly discussed. The rest of the course is devoted to a microscopic theory of superconductivity.

Table 1.1: Parameters for metallic superconductors

	$T_c$ , K	$H_c$ , Oe	$H_{c2}$ , Oe	$\lambda_L$ , Å	$\xi_0$ , Å	$\kappa$	Type
Al	1.18	105		500	16000	0.01	I
Hg	4.15	400		400			I
Nb	9.25	1600	2700	470	390	1.2	II
Pb	7.2	800		390	830	0.47	I
Sn	3.7	305		510	2300	0.15	I
In	3.4	300		400	3000		I
V	5.3	1020		400	~300	~ 0.7	II

Table 1.2: Parameters for some high temperature superconductors

	$T_c$ , K	$H_{c2}$ , T	$\lambda_L$ , Å	$\xi_0$ , Å	$\kappa$	Type
Nb <sub>3</sub> Sn	18	25	~2000	115		II
La <sub>0.925</sub> Sr <sub>0.072</sub> CuO <sub>4</sub>	34		1500	20	75	II
YBa <sub>2</sub> Cu <sub>3</sub> O <sub>7</sub>	92.4	150	2000	15	140	II
Bi <sub>2</sub> Sr <sub>2</sub> Ca <sub>3</sub> CuO <sub>10</sub>	111					II
Tl <sub>2</sub> Sr <sub>2</sub> Ca <sub>2</sub> Cu <sub>3</sub> O <sub>10</sub>	123					II
HgBa <sub>2</sub> Ca <sub>2</sub> Cu <sub>3</sub> O <sub>8</sub>	133					II
MgB <sub>2</sub>	36.7	14	1850	50	40	II

## 1.2 The London model

We assume that the current flows without dissipation and has the form

$$\mathbf{j}_s = n_s e \mathbf{v}_s$$

whence the velocity of superconducting electrons is  $\mathbf{v}_s = \mathbf{j}/n_s e$  where  $n_s$  is their density. Now we come to the most important argument [F. London and H. London, 1935]: Being non-dissipative, this current contributes to the kinetic energy of superconducting electrons. The total free energy is a sum of the kinetic energy of superconducting electrons and the magnetic energy

$$\mathcal{F} = \int \left[ \frac{n_s m \mathbf{v}_s^2}{2} + \frac{\mathbf{h}^2}{8\pi} \right] dV = \int \left[ \frac{m \mathbf{j}_s^2}{2n_s e^2} + \frac{\mathbf{h}^2}{8\pi} \right] dV .$$

Here  $\mathbf{h}$  is the “microscopic” magnetic field. Its average over large area in the sample gives the magnetic induction  $\mathbf{B}$ . Using the Maxwell equation

$$\mathbf{j}_s = (c/4\pi) \text{curl } \mathbf{h} , \quad (1.1)$$

we transform this to the following form

$$\mathcal{F} = \int \left[ \frac{mc^2}{32\pi^2 n_s e^2} (\text{curl } \mathbf{h})^2 + \frac{\mathbf{h}^2}{8\pi} \right] dV = \frac{1}{8\pi} \int dV \left[ \mathbf{h}^2 + \lambda_L^2 (\text{curl } \mathbf{h})^2 \right] . \quad (1.2)$$

Here

$$\lambda_L = \left( \frac{mc^2}{4\pi n_s e^2} \right)^{\frac{1}{2}} \quad (1.3)$$

is called the London penetration depth. In equilibrium, the free energy is minimal with respect to distribution of the magnetic field. Variation with respect to  $\mathbf{h}$  gives

$$\begin{aligned} \delta \mathcal{F} &= \frac{1}{4\pi} \int dV \left[ \mathbf{h} \cdot \delta \mathbf{h} + \lambda_L^2 (\nabla \times \mathbf{h}) \cdot (\nabla \times \delta \mathbf{h}) \right] \\ &= \frac{1}{4\pi} \int dV \left( \mathbf{h} + \lambda_L^2 \nabla \times \nabla \times \mathbf{h} \right) \cdot \delta \mathbf{h} + \frac{1}{4\pi} \int dV \text{div} [\delta \mathbf{h} \times \text{curl } \mathbf{h}] . \end{aligned}$$

Here we use the identity

$$\text{div} [\mathbf{b} \times \mathbf{a}] = \mathbf{a} \cdot [\nabla \times \mathbf{b}] - \mathbf{b} \cdot [\nabla \times \mathbf{a}]$$

and put  $\mathbf{a} = \nabla \times \mathbf{h}$ ,  $\mathbf{b} = \delta \mathbf{h}$ . Looking for a free energy minimum and omitting the surface term we obtain the London equation:

$$\mathbf{h} + \lambda_L^2 \text{curl curl } \mathbf{h} = 0 . \quad (1.4)$$

Since

$$\text{curl curl } \mathbf{h} = \nabla \text{div } \mathbf{h} - \nabla^2 \mathbf{h}$$

and  $\text{div } \mathbf{h} = 0$ , we find

$$\mathbf{h} - \lambda_L^2 \nabla^2 \mathbf{h} = 0 . \quad (1.5)$$

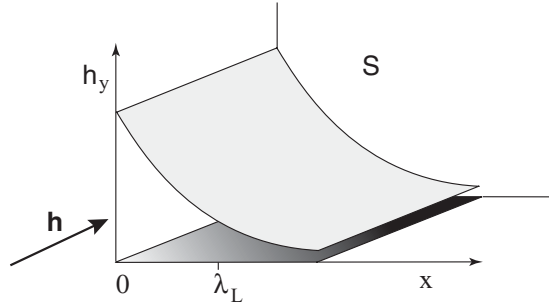


Figure 1.2: The Meissner effect: Magnetic field penetrates into a superconductor only over distances shorter than  $\lambda_L$ .

### 1.2.1 Meissner effect

Equation (1.5) in particular describes the Meissner effect, i.e., an exponential decay of weak magnetic fields and supercurrents in a superconductor. The characteristic length over which the magnetic field decreases is just  $\lambda_L$ . Consider a superconductor which occupies the half-space  $x > 0$ . A magnetic field  $h_y$  is applied parallel to its surface (Fig. 1.2). We obtain from Eq. (1.5)

$$\frac{\partial^2 h_y}{\partial x^2} - \lambda_L^{-2} h_y = 0$$

which gives

$$h_y = h_y(0) \exp(-x/\lambda) .$$

The field decays in a superconductor such that there is no field in the bulk. According to Eq. (1.1) the supercurrent also decays and vanishes in the bulk.

Therefore,

$$\mathbf{B} = \mathbf{H} + 4\pi\mathbf{M} = 0$$

in a bulk superconductor, where  $\mathbf{H}$  is the applied field. The magnetization and susceptibility are

$$\mathbf{M} = -\frac{\mathbf{H}}{4\pi}; \quad \chi = \frac{\partial M}{\partial H} = -\frac{1}{4\pi} \quad (1.6)$$

as for an ideal diamagnetic: Superconductor repels magnetic field lines. The Meissner effect in type I superconductors persists up to the field  $H = H_c$  (see Table 1.1, Fig. 1.7, and the section below) above which superconductivity is destroyed. Type II superconductors display the Meissner effect up to much lower fields, after which vortices appear (see Section 1.5).

### 1.3 Phase coherence

The particle mass flow is determined by the usual quantum-mechanical expression for the momentum per unit volume

$$\mathbf{j}_m = -\frac{i\hbar}{2} [\psi^* \nabla \psi - \psi \nabla \psi^*] = \hbar |\psi|^2 \nabla \chi. \quad (1.7)$$

In order to have a finite current in the superconductor it is necessary that  $\psi$  is the wave function of all the superconducting electrons with a definite phase  $\chi$ : the superconducting electrons should all be in a single quantum state. According to the present understanding what happens is that the electrons (Fermi particles) combine into pairs (Cooper pairs, see the next Chapter) which are Bose objects and condense into a Bose condensate. The current appears when the phase  $\chi$  of the condensate function  $\psi$  slowly varies in space. Equation (1.7) suggests that  $\mathbf{P} = \hbar \nabla \chi$  is the momentum of a condensate particle (which is a pair in the superconductor). For charged particles, the momentum is  $\mathbf{p} = \mathbf{P} - (e^*/c)\mathbf{A}$  where  $\mathbf{P}$  is the canonical momentum,  $\mathbf{A}$  is the vector potential of the magnetic field, and  $e^*$  is the charge of the carrier. In superconductors the charge is carried by pairs of electrons thus  $e^* = 2e$  and the Cooper pair mass is  $2m$ .

Using the definition of the momentum we introduce the velocity of superconducting electrons

$$\mathbf{v}_s = \frac{\hbar}{2m} \left( \nabla \chi - \frac{2e}{\hbar c} \mathbf{A} \right). \quad (1.8)$$

Now the electric current becomes

$$\mathbf{j}_s = n_s e \mathbf{v}_s = -\frac{e^2 n_s}{mc} \left( \mathbf{A} - \frac{\hbar c}{2e} \nabla \chi \right). \quad (1.9)$$

where  $|\psi|^2 = n_s/2$  is the density of electron pairs.

It is instructive to compare this equation with Eqs. (1.1) and (1.4). We find from these

$$\text{curl } \mathbf{j} = \frac{c}{4\pi} \text{curl curl } \mathbf{h} = -\frac{c}{4\pi \lambda_L^2} \mathbf{h} = -\frac{c}{4\pi \lambda_L^2} \text{curl } \mathbf{A}$$

Therefore,

$$\mathbf{j} = -\frac{c}{4\pi \lambda_L^2} (\mathbf{A} - \nabla \phi) = -\frac{e^2 n_s}{mc} (\mathbf{A} - \nabla \phi)$$

where  $\nabla \phi$  is a gradient of some function. It is seen that this coincides with Eq. (1.9) where  $\phi = (\hbar c/2e)\chi$ .

#### 1.3.1 Magnetic flux quantization

Let us consider an non-singly-connected superconductor with dimensions larger than  $\lambda_L$  placed in a magnetic field (Fig. 1.3). We choose a contour which goes

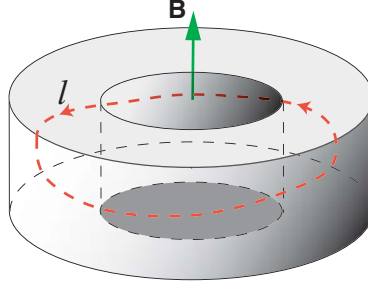


Figure 1.3: Magnetic flux through the hole in a superconductor is quantized.

all the way inside the superconductor around the hole and calculate the contour integral

$$\oint \left( \mathbf{A} - \frac{\hbar c}{2e} \nabla \chi \right) \cdot d\mathbf{l} = \int_S \text{curl } \mathbf{A} \cdot d\mathbf{S} - \frac{\hbar c}{2e} \Delta \chi = \Phi - \frac{\hbar c}{2e} 2\pi n . \quad (1.10)$$

Here  $\Phi$  is the magnetic flux through the contour. The phase change along the closed contour is  $\Delta \chi = 2\pi n$  where  $n$  is an integer because the wave function  $\psi$  is single valued. Since  $\mathbf{j} = 0$  in the bulk, the l.h.s. of Eq. (1.10) vanishes, and we obtain  $\Phi = \Phi_0 n$  where

$$\Phi_0 = \frac{\pi \hbar c}{e} \approx 2.07 \cdot 10^{-7} \text{ Oe} \cdot \text{cm}^2 \quad (1.11)$$

is the quantum of magnetic flux. In SI units,  $\Phi_0 = \pi \hbar / e$ .

### 1.3.2 Coherence length and the energy gap

Cooper pairs keep their correlation within a certain distance called the coherence length  $\xi$  (see the next Chapter). This length introduces an important energy scale. To see this let us argue as follows. Since the correlation of pairs is restricted within  $\xi$  the phase gradient  $\nabla \chi$  cannot exceed  $1/\xi$ ; thus the superconducting velocity cannot be larger than the critical value

$$v_c = \frac{\hbar}{\alpha m \xi} . \quad (1.12)$$

where  $\alpha \sim 1$  is a constant. Thus the energy of a correlated motion of a pair is restricted to  $\Delta_0 \sim p_F v_c = \hbar v_F / \alpha \xi$ . This gives

$$\xi \sim \frac{\hbar v_F}{\Delta_0} .$$

The quantity  $\Delta_0$  is in fact the value of the energy gap  $\Delta(0)$  at zero temperature in the single-particle excitation spectrum in the superconducting state.

We shall see from the microscopic theory in the next Chapter that the energy of excitations

$$\epsilon = \sqrt{\left(\frac{p^2}{2m} - E_F\right)^2 + \Delta^2}$$

cannot be smaller than a certain value  $\Delta$  that generally depends on temperature.

The coherence length is usually defined as

$$\xi_0 = \frac{\hbar v_F}{2\pi k_B T_c}$$

where  $\Delta_0 = 1.76k_B T_c$  and  $\xi_0$  is the coherence length at zero temperature of a clean (without impurities) material. In alloys with  $\ell < \xi_0$ ,

$$\xi = \sqrt{\xi_0 \ell}$$

where  $\ell$  is the mean free path.

The ratio

$$\kappa = \frac{\lambda_L}{\xi}$$

is called the Ginzburg–Landau parameter. Its magnitude separates all superconductors between type-I ( $\kappa < 1/\sqrt{2} \approx 0.7$ ) and type-II ( $\kappa > 1/\sqrt{2}$ ) superconductors. For alloys with  $\ell < \xi_0$

$$\kappa = 0.75 \frac{\lambda_0}{\ell}$$

where  $\lambda_0$  is the London length in a clean material at zero temperature. The conclusion is that alloys are type-II superconductors. Values of  $\lambda_L$ ,  $\xi_0$ , and  $\kappa$  for some materials are listed in Tables 1.1 and 1.2.

## 1.4 Critical currents and magnetic fields

### 1.4.1 Condensation energy

The kinetic energy density of condensate (superconducting) electrons cannot exceed

$$F_c = \frac{n_s m v_c^2}{2} = \frac{n_s \hbar^2}{2\alpha^2 m \xi^2}. \quad (1.13)$$

If the velocity  $v_s$  increases further, the kinetic energy exceeds the energy gain of the superconducting state with respect to the normal state  $F_n - F_s$ , and superconductivity disappears. Therefore,  $F_c = F_n - F_s$  is just this energy gain which is called the condensation energy.

Assume now that the superconductor is placed in a magnetic field  $H$ . It repels the field thus increasing the energy of the external source that creates the field. The energy of the entire system increases and becomes

$$F = F_s + \frac{H^2}{8\pi} = F_n - F_c + \frac{H^2}{8\pi}.$$

In the superconducting state,  $F < F_n$ . When the energy reaches the energy of a normal state  $F_n$ , the superconductivity becomes no longer favorable energetically. Thus the thermodynamic critical magnetic field satisfies

$$F_c = \frac{H_c^2}{8\pi}.$$

Using the expression for  $\lambda_L$  we find from Eq.(1.13)

$$H_c = \frac{\hbar c}{\alpha e \lambda_L \xi} = \frac{\Phi_0}{\alpha \pi \lambda_L \xi}$$

The exact expression for  $H_c$  at temperatures close to  $T_c$  is

$$H_c = \frac{\Phi_0}{2\sqrt{2}\pi\lambda_L\xi} \quad (1.14)$$

Values of  $H_c$  for some materials are given in Table 1.1.

### 1.4.2 Critical currents

There may be several mechanisms of destruction of superconductivity by a current flowing through it.

Mechanism 1. Large type-I samples: The critical current  $I_c$  creates  $H_c$  at the sample surface. For a cylinder with a radius  $R$ ,

$$2\pi R H_c = \frac{4\pi}{c} I_c.$$

If  $R \gg \lambda_L$ , the current flows only within the layer of a thickness  $\lambda_L$  near the sample surface. Thus  $I_c = 2\pi R \lambda_L j_c$  and

$$j_c = \frac{c H_c}{4\pi \lambda_L}. \quad (1.15)$$

Mechanism 2. If the transverse dimensions of the superconductor  $a$  and  $b$  are small,  $a, b \ll \lambda_L$  the current is distributed uniformly over the cross section of the sample. In this case, the dominating mechanism is the pair-breaking: superconductivity is destroyed by the high velocity of superconducting electrons. The critical current is

$$j_c = n_s e v_c = n_s e \hbar / \alpha m \xi. \quad (1.16)$$

In fact, this current density coincides with the critical current in thick samples. Indeed, inserting  $H_c$  and  $\lambda_L$  in Eq. (1.15) we obtain Eq. (1.16). However, the magnetic field created at the surface  $H \sim (c/4\pi)j_c a^2/a \sim (a/\lambda_L)H_c$  is smaller than  $H_c$ . The critical current in Eqs. (1.15), (1.16) is very high. For  $H_c = 500$  Oe and  $\lambda_L = 500 \text{ \AA}$  it can be as high as  $10^8 \text{ A/cm}^2$ .

In type-II superconductors, critical magnetic fields and currents are associated with *quantized vortices*.

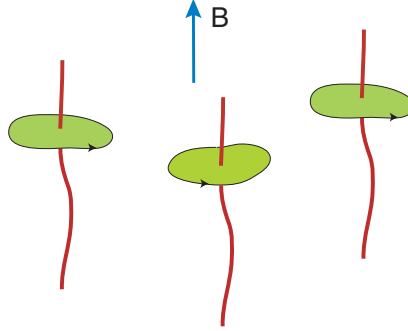


Figure 1.4: Singular lines in a SC with  $2\pi n$  phase variations around them.

## 1.5 Quantized vortices

### 1.5.1 Basic concepts

Consider a type-II superconductor where the London length is large. The supercurrent and magnetic field do not vanish within the region of the order of  $\lambda$  from the surface: there exists a sizable region of nonzero  $v_s$ . If the magnetic field is large enough,  $v_s$  can reach high values,  $v_s \sim (e/mc)Hr$ . For fields  $H \sim \hbar c/e\xi^2$ , the velocity can reach  $r\hbar/m\xi^2 \gg v_c$  for  $r \gg \xi$ . This would lead to destruction of superconductivity if there were no means for compensating a large contribution to  $v_s$  due to the magnetic field.

Assume that we have a linear singularity such that the phase  $\chi$  of the wave function of superconducting electrons  $\psi$  changes by  $2\pi n$  if one goes around this lines along a closed contour, see Fig. 1.4. Consider again the integral along this contour

$$\begin{aligned} -\frac{mc}{e} \oint \mathbf{v}_s \cdot d\mathbf{l} &= \oint \left( \mathbf{A} - \frac{\hbar c}{2e} \nabla \chi \right) \cdot d\mathbf{l} = \int_S \text{curl } \mathbf{A} \cdot d\mathbf{S} - \frac{\hbar c}{2e} \Delta \chi \\ &= \Phi - \frac{\hbar c}{2e} 2\pi n = \Phi - \Phi_0 n . \end{aligned} \quad (1.17)$$

Here  $\Phi$  is the magnetic flux through the contour,  $\Phi_0$  is the flux quantum. The phase change along the closed contour is  $\Delta \chi = 2\pi n$ . We observe that the superconducting velocity increase is completely compensated by the phase variation if the magnetic flux is  $\Phi = \Phi_0 n$ . One can thus expect that in superconductors with large  $\lambda_L$  in high magnetic fields, there will appear linear singularities with a surface density  $n_L$  such that  $(\Phi_0 n_L)$  is equal to the magnetic induction  $B$ . Under these conditions, the superconducting velocity does not increase with distance, and superconductivity is conserved on average.

Each singularity of the phase can exist if the wave function of the superconducting electrons, i.e., the density of superconducting electrons  $n_s = 2|\psi|^2$  goes to zero at the singular line. The size of the region where  $n_s$  is decreased with

respect to its equilibrium value has a size of the order of the coherence length  $\xi$  and is called the vortex core. Such singular objects are called quantized vortices: each vortex carries a quantized magnetic flux  $\Phi_0 n$ . The condition required for existence of vortices is  $\lambda > \xi$  or exactly  $\kappa > 1/\sqrt{2}$ . More favorable energetically are singly quantized vortices which carry one magnetic flux quantum and have a phase circulation  $2\pi$  around the vortex axis.

Vortices are the objects which play a very special role in superconductors and superfluids. In superconductors, each vortex carries exactly one magnetic-flux quantum. Being magnetically active, vortices determine the magnetic properties of superconductors. In addition, they are mobile if the material is homogeneous. In fact, a superconductor in the vortex state is no longer superconducting in a usual sense. Indeed, there is no complete Meissner effect: some magnetic field penetrates into the superconductor via vortices. In addition, regions with the normal phase appear: since the order parameter turns to zero at the vortex axis and is suppressed around each vortex axis within a vortex core with a radius of the order of the coherence length, there are regions with a finite low-energy density of states. Moreover, mobile vortices come into motion in the presence of an average (transport) current. This produces dissipation and causes a finite resistivity (the so-called flux flow resistivity): a superconductor is no longer “superconducting”.

To avoid motion of vortices and thus ensure zero resistance of a superconductor, various defects such as granular structure, lattice defects, artificial defects are introduced into the superconducting material. These defects attract vortices, or “pin” them in the superconductor. To overcome the pinning force one has to apply a finite current density, critical depinning current  $j_c$ , that produces the Lorentz force

$$\mathbf{F}_L = \frac{\Phi_0}{c} [\mathbf{j}_c \times \hat{\mathbf{z}}]$$

where  $\hat{\mathbf{z}}$  is the unit vector in the direction of the magnetic field. Depending on the material, the critical current can be as high as  $10^4 \div 10^5$  A/cm<sup>2</sup>. For currents below the depinning current, a type-II superconductor can have zero resistance up to very high magnetic fields  $H_{c2}$  which are considerably higher than  $H_c$  (see below).

In superfluids, vortices appear in a container with helium rotating at an angular velocity  $\Omega$  above a critical value which is practically not high and can easily be reached in experiment. Vortices are also created if a superfluid flows in a tube with a sufficiently high velocity. The driving force that pushes vortices is now the Magnus force. Vortices move and experience reaction from the normal component; this couples the superfluid and normal components and produces a “mutual friction” between them. As a result, the superflow is no longer persistent.

### 1.5.2 Vortices in the London model

Let us take curl of Eq. (1.9). We find

$$\mathbf{h} - \frac{\hbar c}{2e} \text{curl} \nabla \chi = -\frac{mc}{n_s e^2} \text{curl} \mathbf{j}_s = -\lambda_L^2 \text{curl} \text{curl} \mathbf{h} .$$

This looks like Eq. (1.5) except for one extra term. This term is nonzero if there are vortices. In the presence of vortices, the London equation should be modified. For an  $n$ -quantum vortex we have

$$\text{curl} \nabla \chi = 2\pi n \hat{\mathbf{z}} \delta^{(2)}(\mathbf{r})$$

where  $\hat{\mathbf{z}}$  is the unit vector in the direction of the vortex axis. Therefore, the London equation for a vortex becomes

$$\mathbf{h} + \lambda_L^2 \text{curl} \text{curl} \mathbf{h} = n \Phi_0 \delta^{(2)}(\mathbf{r}) \quad (1.18)$$

where  $\Phi_0$  is the vector along the vortex axis with the magnitude of one flux quantum. For a system of vortices

$$\mathbf{h} + \lambda_L^2 \text{curl} \text{curl} \mathbf{h} = n \Phi_0 \sum_k \delta^{(2)}(\mathbf{r} - \mathbf{r}_k) \quad (1.19)$$

where the sum is over all the vortex positions  $\mathbf{r}_k$ .

One can easily find the magnetic field for a single straight vortex (see Problem 1.1). In cylindrical coordinates  $\mathbf{h} = (0, 0, h_z(r))$ , the magnetic field is

$$h_z(r) = \frac{n \Phi_0}{2\pi \lambda_L^2} \ln \left( \frac{\lambda_L}{r} \right)$$

near the vortex axis  $r \ll \lambda_L$ . The magnetic field increases logarithmically near the vortex axis. However, in our model, the coordinate  $r$  cannot be made shorter than the coherence length since  $n_s$  vanishes at the vortex axis, and the London equation does not apply for  $r < \xi$ . Therefore, at the axis

$$h(0) = \frac{n \Phi_0}{2\pi \lambda_L^2} \ln \left( \frac{\lambda_L}{\xi} \right) .$$

We can calculate the current around the vortex near the core.

$$j_\phi = \frac{c}{4\pi} \frac{\partial h_z}{\partial r} = \frac{nc \Phi_0}{8\pi^2 \lambda_L^2 r} = \frac{n_s e n \hbar}{2mr}$$

For a single-quantum vortex the superconducting velocity is

$$v_{s,\phi} = \frac{\hbar}{2mr}$$

Therefore, the phase is just the azimuthal angle:

$$\chi = \phi$$

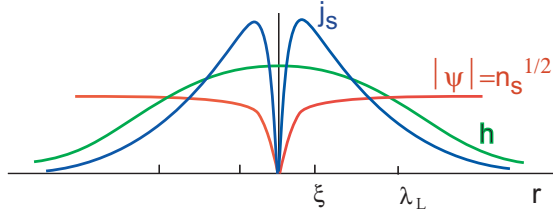


Figure 1.5: Structure of a single vortex. The core region with the radius  $\xi$  is surrounded by currents. Together with the magnetic field, they decay at distances of the order of  $\lambda_L$ .

### 1.5.3 Critical fields in type-II superconductors

The free energy of a single-quantum vortex per unit length is

$$\begin{aligned}\mathcal{F} &= \frac{1}{8\pi} \int [\mathbf{h}(\mathbf{h} + \lambda_L^2 \text{curl curl } \mathbf{h}) + \text{div}[\mathbf{h} \times \text{curl } \mathbf{h}]] d^2r \\ &= \frac{1}{8\pi} \int h_z \Phi_0 \delta^{(2)}(r) d^2r + \frac{1}{8\pi} \int [\mathbf{h} \times \text{curl } \mathbf{h}] dl.\end{aligned}\quad (1.20)$$

The last integral is taken along a remote contour and vanishes. The first integral gives

$$\mathcal{F}_L = \frac{\Phi_0^2}{16\pi^2 \lambda_L^2} \ln \frac{\lambda_L}{\xi} = \frac{\hbar^2 \pi n_s}{4m} \ln \frac{\lambda_L}{\xi}.\quad (1.21)$$

For an  $n$ -quantum vortex we would obtain

$$\mathcal{F}_L = \frac{n^2 \Phi_0^2}{16\pi^2 \lambda_L^2} \ln \left( \frac{\lambda_L}{\xi} \right).\quad (1.22)$$

The energy is proportional to  $n^2$ . Therefore, vortices with  $n > 1$  are not favorable: The energy of  $n$  single-quantum vortices is proportional to the first power of  $n$  and is thus smaller than the energy of one  $n$ -quantum vortex.

Equation (1.21) allows to find the lower critical magnetic field, i.e., the field  $H$  above which the first vortex appears. The free energy of a unit volume of a superconductor with a set of single-quantum vortices is  $F_L = n_L \mathcal{F}_L = (B/\Phi_0) \mathcal{F}_L$ . The proper thermodynamic potential in an external field  $\mathbf{H}$  is the Gibbs free energy  $G = F - \mathbf{H}\mathbf{B}/4\pi$

$$G = \frac{B\mathcal{F}_L}{\Phi_0} - \frac{BH}{4\pi} = \frac{B\Phi_0}{16\pi^2 \lambda_L^2} \ln \left( \frac{\lambda_L}{\xi} \right) - \frac{BH}{4\pi}.$$

If  $H < H_{c1}$  where

$$H_{c1} = \frac{\Phi_0}{4\pi \lambda_L^2} \ln \left( \frac{\lambda_L}{\xi} \right),\quad (1.23)$$

the Gibbs free energy is minimal for  $B = 0$ . This corresponds to zero field in the bulk: the Meissner effect takes place. The free energy becomes negative if

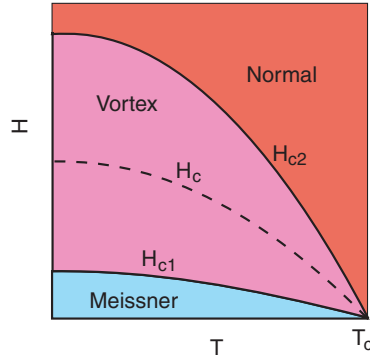


Figure 1.6: Phase diagram of a type II superconductor

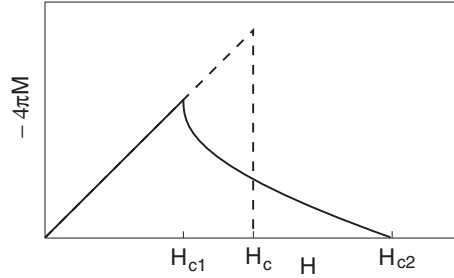


Figure 1.7: Full line: Magnetization of a type II superconductor. The linear part at low fields corresponds to the full Meissner effect Eq. (1.6). Dashed line: Magnetization of a type I superconductor. The Meissner effect persists up to the thermodynamic critical field  $H_c$ .

$H > H_{c1}$ . Therefore, it decreases with increasing  $B$  inside the superconductor. This means that vortices appear for  $H > H_{c1}$ .

As the magnetic field increases, vortices become more and more dense, and the normal phase in the cores occupies larger and larger fraction of the sample. The superconductivity is totally destroyed when their cores start to overlap, i.e., when their density  $n_L = B/\Phi_0 \sim 1/\pi\xi^2$ . The exact condition is

$$H_{c2} = \frac{\Phi_0}{2\pi\xi^2}.$$

Using Eq. (1.14) we note that

$$H_{c1} = H_c \frac{\ln \kappa}{\sqrt{2}\kappa}; \quad H_{c2} = \sqrt{2}\kappa H_c, \quad (1.24)$$

i.e., for superconductors with a large  $\kappa$ , the critical field  $H_{c1}$  is considerably lower than  $H_{c2}$ . At the same time, the upper critical field  $H_{c2}$  is considerably

higher than  $H_c$ .

The phase diagram of a type II superconductor is shown in Fig. 1.6.

For more reading on vortices in type II superconductors see Refs. [5, 6, 7, 8].

## Chapter 2

# The BCS theory

### 2.1 Landau Fermi-liquid

The ground state of a system of Fermions corresponds to the filled states with energies  $E$  below the maximal Fermi energy  $E_F$ , determined by the number of Fermions. In an homogeneous system, one can describe particle states by momentum  $\mathbf{p}$  such that the spectrum becomes  $E_{\mathbf{p}}$ . The condition of maximum energy  $E_{\mathbf{p}} = E_F$  defines the Fermi surface in the momentum space. In an isotropic system, this is a sphere such that its volume divided by  $(2\pi\hbar)^3$

$$n_{\alpha} = \frac{4\pi p_F^3}{3(2\pi\hbar)^3}$$

gives number of particles with the spin projection  $\alpha$  per unit (spatial) volume of system. For electrons with spin  $\frac{1}{2}$ , the total number of particles in the unit volume of the system, i.e., the particle density is twice  $n_{\alpha}$

$$n = \frac{p_F^3}{3\pi^2\hbar^3} \quad (2.1)$$

This ground state corresponds to a ground-state energy  $E_0$ .

Excitations in the Fermi liquid that increase its energy as compared to  $E_0$  are created by moving a particle from a state below the Fermi surface to a state above it. This process can be considered as a superposition of two processes. First is a removal of a particle from the system out of a state below the Fermi surface. The second is adding a particle to a state above the Fermi surface. By taking a particle out of the state with an energy  $E_1 < E_F$  we increase the energy of the system and create a hole excitation with a positive energy  $\epsilon_1 = E_F - E_1$ . By adding a particle into a state with an energy  $E_2 > E_F$  we again increase the energy and create a particle excitation with a positive energy  $\epsilon_2 = E_2 - E_F$ . The energy of the system is thus increased by  $\epsilon_1 + \epsilon_2 = E_2 - E_1$ .

Shown in Fig. 2.1 are processes of creation of particle and hole excitations in a Fermi liquid. Consider it in more detail. Removing a particle with a

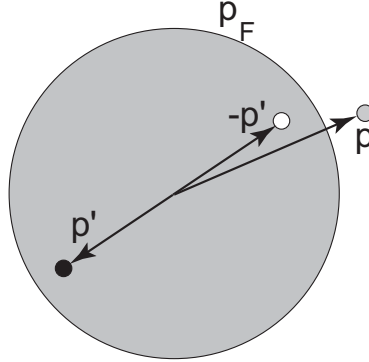


Figure 2.1: Particle (shaded circle) and hole (white circle) excitations in Landau Fermi liquid. The particle excitation is obtained by adding a particle. The hole excitation is obtained by removing a particle (black circle) with an opposite momentum.

momentum  $\mathbf{p}'$  and an energy  $E'$  from below the Fermi surface,  $p' < p_F$  and  $E' < E_F$ , creates an excitation with a momentum  $-\mathbf{p}'$  and an energy  $\epsilon_{-\mathbf{p}'} = E_F - E'$ . Adding a particle with a momentum  $\mathbf{p}$  and energy  $E$  above the Fermi surface,  $p > p_F$  and  $E > E_F$ , creates an excitation with momentum  $\mathbf{p}$  and energy  $\epsilon_{\mathbf{p}} = E - E_F$ . For an isotropic system, the excitation spectrum will thus have the form

$$\epsilon_{\mathbf{p}} = \begin{cases} \frac{p^2}{2m} - E_F, & p > p_F \\ E_F - \frac{p^2}{2m}, & p < p_F \end{cases} \quad (2.2)$$

shown in Fig. 2.2.

The particle and hole excitations live in a system of Fermions where a strong correlation exists due to the Pauli principle. How well elementary excitations with a free-particle spectrum Eq. (2.2) are defined here?

One can show that uncertainty of the quasiparticle energy due to quasiparticle-quasiparticle scattering,  $\delta\epsilon \sim \hbar P$ , where  $P$  is the probability of scattering, in 2 dimensional and 3 dimensional systems is small compared to the energy if  $\epsilon \ll E_F$ , i.e., near the Fermi surface. In other words, quasiparticles are well defined only near the Fermi surface. For a one dimensional system, however, the situation is different, and the Landau quasiparticles do not exist. The one-dimensional system of Fermions is known as the Luttinger liquid, which is beyond the present course.

Let us now define the Hamiltonian for particles and holes. For particles, we define a single-electron Hamiltonian

$$\hat{H}_e = \frac{1}{2m} \left( -i\hbar\nabla - \frac{e}{c}\mathbf{A} \right)^2 + U(\mathbf{r}) - \mu \quad (2.3)$$

where  $\mu$  is the chemical potential and  $U(\mathbf{r})$  is some potential energy. In the normal state,  $\mu = E_F$ . Being applied to a system of totally  $\mathcal{N} = \int n dV$

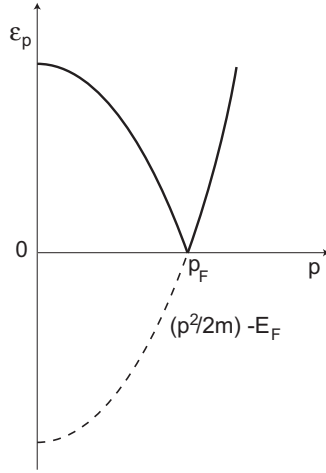


Figure 2.2: Single-particle spectrum  $(p^2/2m) - E_F$  (dashed line) is transformed into the Landau excitation spectrum  $\epsilon_{\mathbf{p}}$  in a strongly correlated Fermi liquid.

particles, it will produce a Hamiltonian in the form  $\mathcal{H} - \mu\mathcal{N}$  where  $\mathcal{H}$  is the Hamiltonian of the full system. This is more appropriate for a system where the chemical potential is fixed rather than the number of particles, as is the case, for example, in superconductors connected to an external circuit. The Hamiltonian Eq. (2.3) corresponds to the canonical momentum operator  $\hat{\mathbf{P}} = -i\hbar\nabla$  and is assumed to be spin independent.

The wave function of a particle excitation  $u_{\epsilon,\mathbf{p}}(\mathbf{r})$  with an energy  $\epsilon$  and momentum  $\mathbf{p}$  satisfies

$$\hat{H}_e u_{\epsilon,\mathbf{p}}(\mathbf{r}) = \epsilon_{\mathbf{p}} u_{\epsilon,\mathbf{p}}(\mathbf{r}) \quad (2.4)$$

Let us now turn to hole excitations. The hole wave function  $v_{\epsilon,\mathbf{p}}(\mathbf{r})$  with an energy  $\epsilon$  and momentum  $\mathbf{p}$  satisfies

$$\hat{H}_h v_{\epsilon,\mathbf{p}}(\mathbf{r}) = \epsilon_{\mathbf{p}} v_{\epsilon,\mathbf{p}}(\mathbf{r})$$

A hole excitation is the absence of a particle with the energy  $-\epsilon$  and momentum  $-\mathbf{p}$ . According to the Landau Fermi-liquid description, the hole Hamiltonian is thus

$$\hat{H}_h = -\hat{H}_e^*$$

The Hamiltonian

$$\hat{H}_e^* = \frac{1}{2m} \left( i\hbar\nabla - \frac{e}{c} \mathbf{A} \right)^2 + U(\mathbf{r}) - E_F \quad (2.5)$$

corresponds to the canonical momentum operator  $-\hat{\mathbf{P}} = i\hbar\nabla$ . The hole wave function thus satisfies

$$\hat{H}_e^* v_{\epsilon,\mathbf{p}}(\mathbf{r}) = -\epsilon_{\mathbf{p}} v_{\epsilon,\mathbf{p}}(\mathbf{r}) \quad (2.6)$$

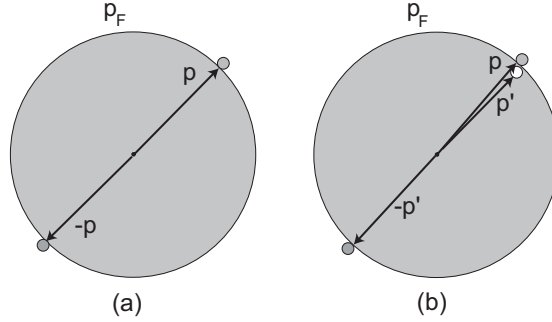


Figure 2.3: (a) A Cooper pair is formed out of a particle excitation with a momentum  $\mathbf{p}$  and that with a momentum  $-\mathbf{p}$  above the Fermi surface (shaded circles), which is equivalent to (b) a particle excitation with a momentum  $\mathbf{p}$  and a removed hole excitation (white circle) with nearly the same momentum  $\mathbf{p}'$ .

## 2.2 The Cooper problem

The original Cooper problem is as follows. Consider an object which is made out of a pair of electrons with energies  $\epsilon_{\mathbf{p}}$  having opposite spins and opposite momenta  $\mathbf{p}$  and  $-\mathbf{p}$  slightly beyond the Fermi surface, see Fig. 2.3 (a). Their wave functions are  $u_{\mathbf{p}}(\mathbf{r}) = e^{i\mathbf{p}\cdot\mathbf{r}/\hbar}U_{\mathbf{p}}$  and  $u_{-\mathbf{p}}(\mathbf{r}) = e^{-i\mathbf{p}\cdot\mathbf{r}/\hbar}U_{-\mathbf{p}}$ , respectively. We shall see later that the pair is actually formed out of an electron in a state  $u_{\mathbf{p}}(\mathbf{r}) = e^{i\mathbf{p}\cdot\mathbf{r}/\hbar}U_{\mathbf{p}}$  above the Fermi surface and an annihilated hole which was formerly in a state  $v_{\mathbf{p}'}(\mathbf{r}) = e^{i\mathbf{p}'\cdot\mathbf{r}/\hbar}V_{\mathbf{p}'}$  with nearly the same momentum  $\mathbf{p}' \approx \mathbf{p}$  below the Fermi surface. The annihilated hole is in a sense equivalent to an electron with momentum  $-\mathbf{p}'$  and has a wave function  $v_{\mathbf{p}'}^*(\mathbf{r}) = u_{-\mathbf{p}'}(\mathbf{r}) = e^{-i\mathbf{p}'\cdot\mathbf{r}/\hbar}V_{\mathbf{p}'}^*$ , Fig. 2.3 (b).

The pair wave function is

$$\Psi_{\mathbf{p}}^{\text{pair}}(\mathbf{r}_1, \mathbf{r}_2) = u_{\mathbf{p}}(\mathbf{r}_1)u_{-\mathbf{p}}(\mathbf{r}_2) = e^{i\mathbf{p}\cdot(\mathbf{r}_1 - \mathbf{r}_2)/\hbar}U_{\mathbf{p}}V_{\mathbf{p}}^*$$

The linear combination with various  $\mathbf{p}$  gives the coordinate wave function

$$\Psi^{\text{pair}}(\mathbf{r}_1, \mathbf{r}_2) = \sum_{\mathbf{p}} e^{i\mathbf{p}\cdot(\mathbf{r}_1 - \mathbf{r}_2)/\hbar}a_{\mathbf{p}} \quad (2.7)$$

where  $a_{\mathbf{p}} = U_{\mathbf{p}}V_{\mathbf{p}}^*$ . The inverse transformation is

$$a_{\mathbf{p}} = V^{-1} \int \Psi(\mathbf{r})e^{-i\mathbf{p}\cdot\mathbf{r}/\hbar} d^3r$$

where  $V$  is the volume of the system.

Assume that the electrons in the pair interact through the potential  $W(\mathbf{r}_1, \mathbf{r}_2) = W(\mathbf{r}_1 - \mathbf{r}_2)$ . Their Hamiltonian is  $\hat{H}_e(1) + \hat{H}_e(2) + W$ . The Schrödinger equation has the form

$$\left[ \hat{H}_e(\mathbf{r}_1) + \hat{H}_e(\mathbf{r}_2) + W(\mathbf{r}_1, \mathbf{r}_2) \right] \Psi^{\text{pair}}(\mathbf{r}_1, \mathbf{r}_2) = E\Psi^{\text{pair}}(\mathbf{r}_1, \mathbf{r}_2)$$

Multiplying this by  $e^{-i\mathbf{p}(\mathbf{r}_1-\mathbf{r}_2)}$  and calculating the integral over the volume we obtain this equation in the momentum representation,

$$[2\epsilon_{\mathbf{p}} - E_{\mathbf{p}}]a_{\mathbf{p}} = - \sum_{\mathbf{p}_1} W_{\mathbf{p},\mathbf{p}_1} a_{\mathbf{p}_1}$$

where

$$W_{\mathbf{p},\mathbf{p}_1} = V^{-1} \int e^{-i(\mathbf{p}-\mathbf{p}_1)\cdot\mathbf{r}/\hbar} W(\mathbf{r}) d^3r$$

Assume that

$$W_{\mathbf{p},\mathbf{p}_1} = \begin{cases} W/V, & \epsilon_{\mathbf{p}} \text{ and } \epsilon_{\mathbf{p}_1} < E_c \\ 0, & \epsilon_{\mathbf{p}} \text{ or } \epsilon_{\mathbf{p}_1} > E_c \end{cases}$$

where  $E_c \ll E_F$ . The interaction strength  $W \sim W_0 v_0$  where  $W_0$  is the magnitude of the interaction potential while  $v_0 = a_0^3$  is the volume where the interaction of a range  $a_0$  is concentrated. We have

$$a_{\mathbf{p}} = \frac{W}{E - 2\epsilon_{\mathbf{p}}} \frac{1}{V} \sum_{\mathbf{p}_1} a_{\mathbf{p}_1} = \frac{W}{E - 2\epsilon_{\mathbf{p}}} \sum'_{\mathbf{p}_1} a_{\mathbf{p}_1} \quad (2.8)$$

Here the sum  $\sum_{\mathbf{p}}$  is taken over  $\mathbf{p}$  which satisfy  $\epsilon_{\mathbf{p}} < E_c$ , while the sum  $\sum'$  is taken over the states in a unit volume. Let us denote

$$C = \sum'_{\mathbf{p}} a_{\mathbf{p}}$$

Eq. (2.8) yields

$$a_{\mathbf{p}} = \frac{WC}{E - 2\epsilon_{\mathbf{p}}}$$

whence

$$C = WC \sum'_{\mathbf{p}} \frac{1}{E - 2\epsilon_{\mathbf{p}}}$$

This gives

$$\frac{1}{W} = \sum'_{\mathbf{p}} \frac{1}{E - 2\epsilon_{\mathbf{p}}} \equiv \Phi(E) \quad (2.9)$$

Equation (2.9) is illustrated in Fig. 2.4. Let us put our system in a large box. The levels  $\epsilon_{\mathbf{p}}$  will become a discrete set  $\epsilon_n$  shown in Fig. 2.4 by vertical dashed lines. The lowest level  $\epsilon_0$  is very close to zero and will approach zero as the size of the box increases. The function  $\Phi(E)$  varies from  $-\infty$  to  $+\infty$  as  $E$  increases and crosses each  $\epsilon_n > 0$ . However, for negative  $E < 0$ , the function  $\Phi(E)$  approaches zero as  $E \rightarrow -\infty$ , and there is a crossing point with a negative level  $-1/|W|$  for negative  $E$ . This implies that *there is a state with negative energy*  $E_0 < 0$  satisfying Eq. (2.9) for a negative  $W < 0$ .

For an attraction  $W < 0$  we have

$$\frac{1}{|W|} = \sum'_{\mathbf{p}} \frac{1}{2\epsilon_{\mathbf{p}} - E}$$

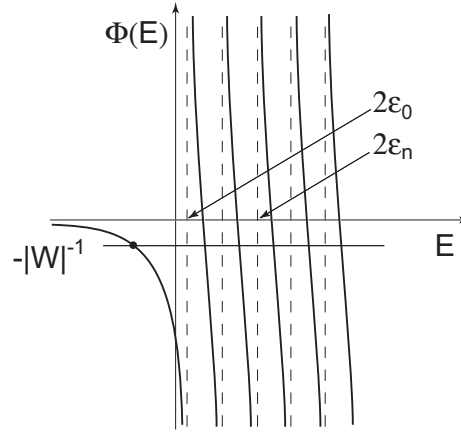


Figure 2.4: The function  $\Phi(E)$  for a system with a discrete spectrum  $\epsilon_n$ .

Let  $n(\epsilon)$  be the number of states within a unit volume per one spin projection with energies below  $\epsilon$ . The quantity

$$N(\epsilon) = \frac{dn(\epsilon)}{d\epsilon}$$

is called the density of states (DOS). In the normal state where  $\epsilon_{\mathbf{p}} = p^2/2m - E_F$ ,

$$n(\epsilon) = \frac{(4/3)\pi p^3}{(2\pi\hbar)^3}$$

Therefore,

$$N(\epsilon) = \frac{mp}{2\pi^2\hbar^3}$$

Having this in mind, we substitute the sum with the integral

$$\sum'_{\mathbf{p}} = 2 \int \frac{d^3p}{(2\pi\hbar)^3} = 2 \int \frac{mp}{2\pi^2\hbar^3} d\epsilon_{\mathbf{p}}$$

the factor 2 accounts for the spin.

Now, for a negative energy  $E = E_0 = -|E_0|$

$$\frac{1}{|W|} = 2 \int_0^{E_c} \frac{mp}{2\pi^2\hbar^3} \frac{d\epsilon_{\mathbf{p}}}{2\epsilon_{\mathbf{p}} - E_0} = 2N(0) \int_0^{E_c} \frac{d\epsilon}{2\epsilon + |E_0|} = N(0) \ln \left( \frac{|E_0| + 2E_c}{|E_0|} \right) \quad (2.10)$$

Here we replace  $p$  with a constant  $p_F$  since  $E_c \ll E_F$  and thus  $|p - p_F| \ll p_F$ . We also denote

$$N(0) = \frac{mp_F}{2\pi^2\hbar^3} \quad (2.11)$$

the density of states at the Fermi surface. Eq. (2.10) yields

$$|E_0| = \frac{2E_c}{e^{1/N(0)|W|} - 1} \quad (2.12)$$

The dimensionless factor  $\lambda \equiv N(0)W \sim N(0)W_0 a_0^3$  is called the interaction constant. For weak coupling,  $N(0)|W| \ll 1$ , we find

$$|E_0| = 2E_c e^{-1/N(0)|W|}$$

For a strong coupling,  $N(0)|W| \gg 1$ ,

$$|E_0| = 2N(0)|W|E_c$$

We see that there exists a state of a particle-hole pair (the Cooper pair) with an energy  $|E_0|$  below the Fermi surface. It means that the system of normal-state particles and holes is unstable towards formation of pairs provided there is an attraction (however small) between electrons: Indeed, if we place a pair of extra electrons in a system which has a filled Fermi surface, these two electrons find a state *below* the Fermi surface, in contradiction to the assumption that there are no more available states inside the Fermi surface.

In conventional superconductors, the attraction is caused by an exchange of phonons. The attraction between electrons can also be caused by magnetic interactions which favors triplet pairing (with a nonzero spin of pair). The Coulomb repulsion is strongly reduced by screening effects at distances of the order of the size of the pair  $\xi$  thus it does not destroy pairing. Fig. 2.5 illustrates the effect on the excitation spectrum of coupling between a particle and a hole near the Fermi surface shown in Fig. 2.3.

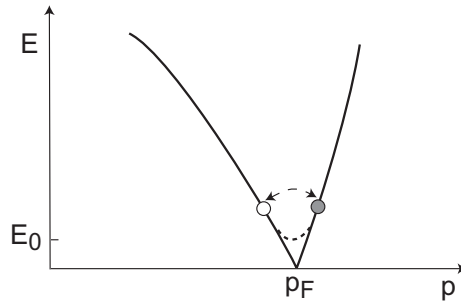


Figure 2.5: The coupling between electron and hole modifies the energy spectrum: The gap equal to  $|E_0|$  opens near the Fermi surface.

This Cooper pairing effect provides a basis for understanding of superconductivity. According to this picture, the pairs, being Bose particles, form a Bose condensate in a single state with a wave function that has a single phase for all pairs, which is the basic requirement for existence of a spontaneous supercurrent.

## 2.3 The BCS model

### 2.3.1 The Bogoliubov–de Gennes equations

Coupling between particles and holes is described by introduction of a pairing field  $\Delta$  into the particle and hole equations (2.4) and (2.6). The resulting equations are known as the *Bogoliubov–de Gennes equations* (BdGE)

$$\hat{H}_e u(\mathbf{r}) + \Delta(\mathbf{r})v(\mathbf{r}) = \epsilon u(\mathbf{r}) \quad (2.13)$$

$$-\hat{H}_e^* v(\mathbf{r}) + \Delta^*(\mathbf{r})u(\mathbf{r}) = \epsilon v(\mathbf{r}) \quad (2.14)$$

The functions  $(u, v)$  are orthogonal

$$\int [u_m^*(\mathbf{r})u_n(\mathbf{r}) + v_m^*(\mathbf{r})v_n(\mathbf{r})] d^3r = \delta_{mn} \quad (2.15)$$

For the momentum representation we have

$$\int [u_{\mathbf{q}_1}^*(\mathbf{r})u_{\mathbf{q}_2}(\mathbf{r}) + v_{\mathbf{q}_1}^*(\mathbf{r})v_{\mathbf{q}_2}(\mathbf{r})] d^3r = (2\pi)^3 \delta(\mathbf{q}_1 - \mathbf{q}_2) \quad (2.16)$$

### 2.3.2 The self-consistency equation

The pairing field  $\Delta$  is proportional to a two-particle wave function,

$$\Delta(\mathbf{r}) = -W \langle \Psi(\mathbf{r}, \downarrow)\Psi(\mathbf{r}, \uparrow) \rangle = W \langle \Psi(\mathbf{r}, \uparrow)\Psi(\mathbf{r}, \downarrow) \rangle \quad (2.17)$$

Here  $\langle \dots \rangle$  denotes a statistical average. One finds

$$\Delta(\mathbf{r}) = W \sum_n (1 - 2f_n) u_n(\mathbf{r})v_n^*(\mathbf{r}) \quad (2.18)$$

where  $f_n$  is the distribution function. In equilibrium, it is the Fermi function

$$f_n = \frac{1}{e^{\epsilon_n/T} + 1}$$

We see that the pairing field  $\Delta$  is a linear combination of pair states made out of particle-like and annihilated hole-like excitations.

## 2.4 Observables

### 2.4.1 Energy spectrum and coherence factors

Consider the case where  $\Delta = |\Delta|e^{i\chi}$  is constant in space, and the magnetic field is absent. The BdGE have the form

$$\left[ -\frac{\hbar^2}{2m}\nabla^2 - \mu \right] u(\mathbf{r}) + \Delta v(\mathbf{r}) = \epsilon u(\mathbf{r}) \quad (2.19)$$

$$-\left[ -\frac{\hbar^2}{2m}\nabla^2 - \mu \right] v(\mathbf{r}) + \Delta^* u(\mathbf{r}) = \epsilon v(\mathbf{r}) \quad (2.20)$$

where  $\mu = \hbar^2 k_F^2 / 2m$ . We look for a solution in the form

$$u = e^{\frac{i}{2}\chi} U_{\mathbf{q}} e^{i\mathbf{q}\cdot\mathbf{r}}, \quad v = e^{-\frac{i}{2}\chi} V_{\mathbf{q}} e^{i\mathbf{q}\cdot\mathbf{r}} \quad (2.21)$$

where  $\mathbf{q}$  is a constant vector. We have

$$\xi_{\mathbf{q}} U_{\mathbf{q}} + |\Delta| V_{\mathbf{q}} = \epsilon_{\mathbf{q}} U_{\mathbf{q}} \quad (2.22)$$

$$-\xi_{\mathbf{q}} V_{\mathbf{q}} + |\Delta| U_{\mathbf{q}} = \epsilon_{\mathbf{q}} V_{\mathbf{q}} \quad (2.23)$$

where

$$\xi_{\mathbf{q}} = \frac{\hbar^2}{2m} [q^2 - k_F^2]$$

The condition of solvability of Eqs. (2.22) and (2.23) gives

$$\epsilon_{\mathbf{q}} = \pm \sqrt{\xi_{\mathbf{q}}^2 + |\Delta|^2} \quad (2.24)$$

According to the Landau picture of Fermi liquid, we consider only energies  $\epsilon > 0$ . The spectrum is shown in Fig. 2.6.

The wave functions  $u$  and  $v$  for a given momentum  $\mathbf{q}$  are found from Eqs. (2.22), (2.24). We have

$$U_{\mathbf{q}} = \frac{1}{\sqrt{2}} \left( 1 + \frac{\xi_{\mathbf{q}}}{\epsilon_{\mathbf{q}}} \right)^{1/2}, \quad V_{\mathbf{q}} = \frac{1}{\sqrt{2}} \left( 1 - \frac{\xi_{\mathbf{q}}}{\epsilon_{\mathbf{q}}} \right)^{1/2} \quad (2.25)$$

Normalization is chosen to satisfy Eq. (2.16).

The energy  $|\Delta|$  is the lowest single-particle excitation energy in the superconducting state.  $2|\Delta|$  corresponds to an energy which is needed to destroy the Cooper pair. Therefore, one can identify  $2|\Delta|$  as the pairing energy as determined by the Cooper problem in the previous Section,  $|E| = 2|\Delta|$ .

Electrons in the pair have velocity  $v_F$ . Therefore, the characteristic momentum (in addition to  $p_F$ ) associated with the pair is  $\delta p \sim |\Delta|/v_F$ . Using the uncertainty principle,  $\delta p R \sim \hbar$ , where  $R$  has a meaning of effective "size" of a Cooper pair, one finds  $R \sim \hbar v_F / |\Delta|$ . This characteristic scale sets up a very important length scale called the coherence length

$$\xi \sim \hbar v_F / |\Delta|.$$

For a given energy, there are two possible values of

$$\xi_{\mathbf{q}} = \pm \sqrt{\epsilon^2 - |\Delta|^2} \quad (2.26)$$

that correspond respectively to particles or holes (see Fig. 2.6).

The quantity

$$\frac{d\epsilon}{d(\hbar q)} = v_g$$

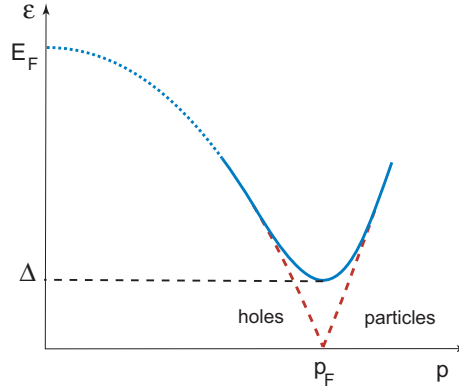


Figure 2.6: The BCS spectrum of excitations in a superconductor. The solid line shows the spectrum of quasiparticles near the Fermi surface where the Landau quasiparticles are well defined. At higher energies closer to  $E_F$  the Landau quasiparticles are not well-defined (dotted line). The dashed line at lower energies shows the behavior of the spectrum in the normal state  $\epsilon = |\xi_{\mathbf{p}}|$ .

is the group velocity of excitations. One has  $q^2 = k_F^2 \pm (2m/\hbar^2)\sqrt{\epsilon^2 - |\Delta|^2}$ . Therefore,

$$v_g = \frac{\hbar q}{m} \frac{\xi_{\mathbf{q}}}{\sqrt{\xi_{\mathbf{q}}^2 + |\Delta|^2}} = v_F \frac{\xi_{\mathbf{q}}}{\sqrt{\xi_{\mathbf{q}}^2 + |\Delta|^2}} = \pm v_F \frac{\sqrt{\epsilon^2 - |\Delta|^2}}{\epsilon} \quad (2.27)$$

where  $v_F = \hbar q/m$  is the velocity at the Fermi surface. We see that the group velocity is positive, i.e., its direction coincides with the direction of  $\mathbf{q}$  for excitations outside the Fermi surface  $\xi_{\mathbf{q}} > 0$ . As we know, these excitations are particle-like. On the other hand,  $v_g < 0$  for excitations inside the Fermi surface  $\xi_{\mathbf{q}} < 0$ , which are known as hole-like excitations.

### 2.4.2 Density of states

Another important quantity is the density of states (DOS)  $N(\epsilon)$  defined as follows. Let us suppose that there are  $n_{\alpha}(q)$  states per spin and per unit volume for particles with momenta up to  $\hbar q$ . The density of states is the number of states within an energy interval from  $\epsilon$  to  $\epsilon + d\epsilon$ , i.e.

$$N(\epsilon) = \frac{dn_{\alpha}(q)}{d\epsilon}$$

As we can see, in a superconductor, there are no excitations with energies  $\epsilon < |\Delta|$ . The DOS per one spin projection is zero for  $\epsilon < |\Delta|$ . For  $\epsilon > |\Delta|$  we have

$$N(\epsilon) = \frac{1}{2} \left| \frac{d}{d\epsilon} \left( \frac{q^3}{3\pi^2} \right) \right| = \frac{q^2}{2\pi^2} \left| \frac{dq}{d\epsilon} \right|^{-1}$$

$$= \frac{mq}{2\pi^2\hbar^2} \frac{\epsilon}{\sqrt{\epsilon^2 - |\Delta|^2}} \approx N(0) \frac{\epsilon}{\sqrt{\epsilon^2 - |\Delta|^2}} \quad (2.28)$$

Here

$$N(0) = \frac{mp_F}{2\pi^2\hbar^3} = \frac{mk_F}{2\pi^2\hbar^2}$$

is the DOS per one spin projection in the normal state for zero energy excitations, i.e., at the Fermi surface. We have replaced here  $q$  with  $k_F$ . Indeed, since  $\Delta \ll E_F$ , the magnitude of  $q$  is very close to  $k_F$  for  $\epsilon \sim \Delta$ . This fact is of a crucial importance for practical applications of the BCS theory, as we shall see in what follows.

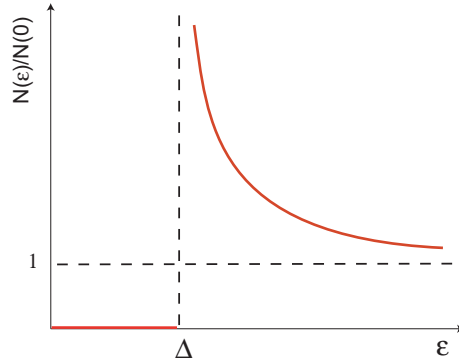


Figure 2.7: The superconducting density of states as a function of energy.

### 2.4.3 The energy gap

For a state Eq. (2.21) specified by a wave vector  $\mathbf{q}$  with  $U_{\mathbf{q}}$  and  $V_{\mathbf{q}}$  from Eq. (2.25) the product  $uv^*$  becomes

$$uv^* = e^{i\chi} U_{\mathbf{q}} V_{\mathbf{q}} = \frac{\Delta}{2\epsilon_{\mathbf{q}}}$$

The self-consistency equation (2.18) yields

$$\Delta = W \sum_{\mathbf{q}} (1 - 2f_{\mathbf{q}}) \frac{\Delta}{2\epsilon_{\mathbf{q}}} \quad (2.29)$$

We replace the sum with the integral

$$\sum_{\mathbf{q}} = \int_{q=0}^{q=\infty} \frac{d^3q}{(2\pi)^3} = \int_{\xi=-E_F}^{\xi=+\infty} \frac{mq}{2\pi^2\hbar^2} d\xi_{\mathbf{q}} \approx N(0) \int_{-\infty}^{+\infty} d\xi_{\mathbf{q}}$$

and notice that, in equilibrium,

$$1 - 2f_{\mathbf{q}} = \tanh\left(\frac{\epsilon_{\mathbf{q}}}{2T}\right)$$

Moreover,

$$\epsilon_{\mathbf{q}} d\epsilon_{\mathbf{q}} = \xi_{\mathbf{q}} d\xi_{\mathbf{q}}$$

When  $\xi$  varies from  $-\infty$  to  $+\infty$ , the energy varies from  $\Delta$  to  $+\infty$  taking each value twice. Therefore, the self-consistency equation takes the form

$$\Delta = W \sum_{\mathbf{q}} (1 - 2f_{\mathbf{q}}) \frac{\Delta}{2\epsilon_{\mathbf{q}}} = N(0)W \int_{|\Delta|}^{\infty} \frac{\Delta}{\sqrt{\epsilon^2 - |\Delta|^2}} \tanh\left(\frac{\epsilon}{2T}\right) d\epsilon \quad (2.30)$$

The integral diverges logarithmically at large energies. In fact, the potential of interaction does also depend on energy  $W = W_{\epsilon}$  in such a way that it vanishes for high energies exceeding some limiting value  $E_c \ll E_F$ . We assume that

$$W_{\epsilon} = \begin{cases} W, & \epsilon < E_c \\ 0, & \epsilon > E_c \end{cases}$$

From Eq. (2.30) we obtain the *gap equation*

$$1 = \lambda \int_{|\Delta|}^{E_c} \frac{1}{\sqrt{\epsilon^2 - |\Delta|^2}} \tanh\left(\frac{\epsilon}{2T}\right) d\epsilon \quad (2.31)$$

where the dimensionless parameter  $\lambda = N(0)W \sim N(0)W_0 a^3$  is called the interaction constant. For phonon mediated electron coupling, the effective attraction works for energies below the Debye energy  $\Omega_D$ . Therefore,  $E_c = \Omega_D$  in Eq. (2.31). This equation determines the dependence of the gap on temperature.

This equation can be used to determine the critical temperature  $T_c$ , at which the gap  $\Delta$  vanishes. We have

$$1 = \lambda \int_0^{E_c} \tanh\left(\frac{\epsilon}{2T_c}\right) \frac{d\epsilon}{\epsilon} \quad (2.32)$$

This reduces to

$$\frac{1}{\lambda} = \int_0^{E_c/2T_c} \frac{\tanh x}{x} dx \quad (2.33)$$

The integral

$$\int_0^a \frac{\tanh x}{x} dx = \ln(aB)$$

Here  $B = 4\gamma/\pi \approx 2.26$  where  $\gamma = e^C \approx 1.78$  and  $C = 0.577\dots$  is the Euler constant. Therefore,

$$T_c = (2\gamma/\pi)E_c e^{-1/\lambda} \approx 1.13E_c e^{-1/\lambda} \quad (2.34)$$

The interaction constant is usually small, being of the order of  $0.1 \div 0.3$  in practical superconductors. Therefore, usually  $T_c \ll E_c$ .

For zero temperature we obtain from Eq. (2.31)

$$\frac{1}{\lambda} = \int_{|\Delta|}^{E_c} \frac{d\epsilon}{\sqrt{\epsilon^2 - |\Delta|^2}} = \text{Arcosh}\left(\frac{E_c}{|\Delta|}\right) \approx \ln(2E_c/|\Delta|) \quad (2.35)$$

Therefore, at  $T = 0$

$$|\Delta| \equiv \Delta(0) = (\pi/\gamma)T_c \approx 1.76T_c$$

### 2.4.4 Current

The quantum mechanical expression for the current density is

$$\begin{aligned} \mathbf{j} = & \frac{e}{2m} \sum_{\alpha} \left\{ \Psi^{\dagger}(\mathbf{r}, \alpha) \left[ \left( -i\hbar\nabla - \frac{e}{c}\mathbf{A} \right) \Psi(\mathbf{r}, \alpha) \right] \right. \\ & \left. + \left[ \left( i\hbar\nabla - \frac{e}{c}\mathbf{A} \right) \Psi^{\dagger}(\mathbf{r}, \alpha) \right] \Psi(\mathbf{r}, \alpha) \right\} \end{aligned} \quad (2.36)$$

In superconducting state we obtain

$$\begin{aligned} \mathbf{j} = & \frac{e}{m} \sum_n \left[ f_n u_n^*(\mathbf{r}) \left( -i\hbar\nabla - \frac{e}{c}\mathbf{A} \right) u_n(\mathbf{r}) \right. \\ & \left. - (1 - f_n) v_n^*(\mathbf{r}) \left( -i\hbar\nabla + \frac{e}{c}\mathbf{A} \right) v_n(\mathbf{r}) + c.c. \right] \end{aligned} \quad (2.37)$$



## Chapter 3

# Andreev reflection

We assume that there are no barriers or other potentials that vary over distances of the order of the electronic wave length  $k_F^{-1}$ . The energy gap should also be smooth over the distances of the order of the electronic wave length. It may, however, vary at distances shorter than the coherence length  $\xi$ . In this case the quasiparticle momentum of the order of  $\hbar k_F$  is a good quantum number such that we can look for a solution in the form

$$\begin{pmatrix} u \\ v \end{pmatrix} = e^{i\mathbf{k}\cdot\mathbf{r}} \begin{pmatrix} U(\mathbf{r}) \\ V(\mathbf{r}) \end{pmatrix} \quad (3.1)$$

where  $|\mathbf{k}| = k_F$  while  $U(\mathbf{r})$  and  $V(\mathbf{r})$  vary slowly over distances of the order of  $k_F^{-1}$ .

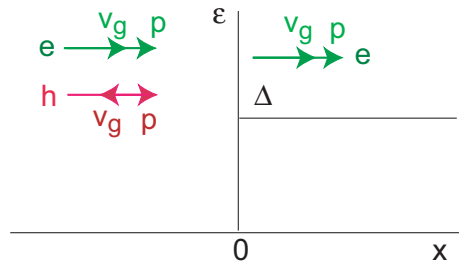


Figure 3.1: The NS structure.

Consider a particle incident from the normal region on the superconducting half-space  $x > 0$  (see Fig. 3.1) with a momentum parallel to the  $x$  axis. Assume that the gap varies over distances longer than the electron wave length  $k_F^{-1}$  and that both the normal metal and the superconductor have the same Fermi velocity, and there are no insulating barriers between them. We assume that the magnetic field is absent. In this case  $\Delta$  and all other potentials depend only

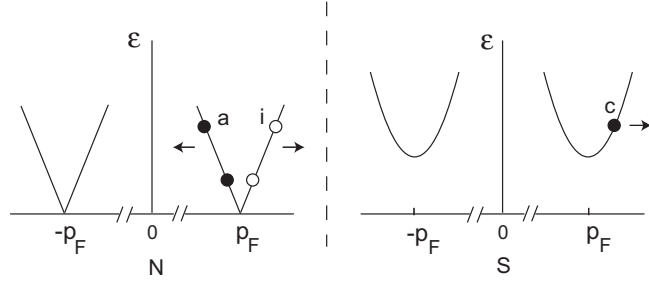


Figure 3.2: The Andreev reflection. If the incident state (i) has an energy above the gap, a transmitted state (c) exists in the superconductor. A particle is partially transmitted and partially reflected back as a hole (a). If the energy is below the gap, there are no states in superconductor, and the particle is fully reflected back as a hole (a).

on one coordinate  $x$  and the BdG equations take the form

$$-\frac{\hbar^2}{2m} \left( \frac{\partial^2}{\partial x^2} + \frac{\partial^2}{\partial y^2} + \frac{\partial^2}{\partial z^2} \right) u - \frac{\hbar^2 k_F^2}{2m} u + \Delta(x)v = \epsilon u \quad (3.2)$$

$$\frac{\hbar^2}{2m} \left( \frac{\partial^2}{\partial x^2} + \frac{\partial^2}{\partial y^2} + \frac{\partial^2}{\partial z^2} \right) v + \frac{\hbar^2 k_F^2}{2m} v + \Delta^*(x)u = \epsilon v \quad (3.3)$$

Consider first the case of high energies  $\epsilon > |\Delta|$ . The particle will penetrate into the superconductor and partially will be reflected back into the normal metal. However, since the gap varies slowly, the reflection process where the momentum is changed such that  $\mathbf{k} \rightarrow -\mathbf{k}$  is prohibited.

In the normal region (on the left) the order parameter decreases to zero at distances shorter than  $\xi$ , so that one can consider  $\Delta = 0$  for  $x < 0$ . The wave functions are

$$\begin{pmatrix} u \\ v \end{pmatrix}_L = e^{i(k_x + \epsilon/\hbar v_x)x + ik_y y + ik_z z} \begin{pmatrix} 1 \\ 0 \end{pmatrix} + a e^{i(k_x - \epsilon/\hbar v_x)x + ik_y y + ik_z z} \begin{pmatrix} 0 \\ 1 \end{pmatrix} \quad (3.4)$$

Here

$$v_x = \hbar k_x / m$$

The wave function thus contains an incident particle [state (i) in Fig. 3.2] and a reflected hole [state (a)]. We choose the coefficient unity in front of the incident wave to ensure the unit density of particles in the incident wave.

The wave function on the right (in the S region) has the form

$$\begin{pmatrix} u \\ v \end{pmatrix}_R = c e^{i(k_x + \lambda_S)x + ik_y y + ik_z z} \begin{pmatrix} U_0 \\ V_0 \end{pmatrix} \quad (3.5)$$

Eqs. (3.2), (3.3) give

$$\lambda_S = \sqrt{\epsilon^2 - |\Delta|^2} / \hbar v_x \quad (3.6)$$

It describes a transmitted particle. The coherence factors  $U_0$  and  $V_0$  are determined by Eq. (2.25):

$$U_0 = \frac{1}{\sqrt{2}} \left[ 1 + \frac{\sqrt{\epsilon^2 - |\Delta|^2}}{\epsilon} \right]^{1/2}, \quad V_0 = \frac{1}{\sqrt{2}} \left[ 1 - \frac{\sqrt{\epsilon^2 - |\Delta|^2}}{\epsilon} \right]^{1/2}$$

They satisfy

$$U_0^2 - V_0^2 = \frac{\sqrt{\epsilon^2 - |\Delta|^2}}{\epsilon}, \quad U_0 V_0 = \frac{|\Delta|}{2\epsilon}$$

The boundary conditions require continuity of the slow functions at the interface whence

$$a = V_0/U_0, \quad c = 1/U_0 \quad (3.7)$$

The coefficient  $a$  describes a process when a particle is reflected as a hole from a spatially non-uniform gap; this process is called the Andreev reflection [9].

For the sub-gap energy  $\epsilon < |\Delta|$ , there are no states below the gap in the S region, thus the wave should decay for  $x > 0$ . The wave function on the right is

$$\begin{pmatrix} u \\ v \end{pmatrix}_R = c e^{(ik_x - \tilde{\lambda}_S)x + ik_y y + ik_z z} \begin{pmatrix} \tilde{U}_0 \\ \tilde{V}_0 \end{pmatrix} \quad (3.8)$$

where

$$\tilde{\lambda}_S = \sqrt{|\Delta|^2 - \epsilon^2}/\hbar v_x \quad (3.9)$$

and

$$\tilde{U}_0 = \frac{1}{\sqrt{2}} \left( 1 + i \frac{\sqrt{|\Delta|^2 - \epsilon^2}}{\epsilon} \right), \quad \tilde{V}_0 = \frac{1}{\sqrt{2}} \left( 1 - i \frac{\sqrt{|\Delta|^2 - \epsilon^2}}{\epsilon} \right)$$

The coefficients are

$$a = \tilde{V}_0/\tilde{U}_0, \quad c = 1/\tilde{U}_0$$

However, now

$$|a|^2 = 1 \quad (3.10)$$

The Andreev reflection is complete since there are no transmitted particles.

The Andreev reflection has an interesting and surprising property. The magnitude squared of the particle momentum in Eq. (3.4) is

$$p^2 = p_x^2 + p_y^2 + p_z^2 = \hbar^2 [(k_x \pm \epsilon/\hbar v_x)^2 + k_y^2 + k_z^2] = \hbar^2 \left[ k_F^2 \pm \frac{2k_x \epsilon}{\hbar v_x} \right] = \hbar^2 k_F^2 \pm 2m\epsilon$$

The total momentum of the incident particle is thus  $p = \hbar k_F + \epsilon/v_F$  such that  $p > p_F$ . Its energy corresponds to the rising (right) part of the spectrum branch [point (i)] in Fig. 3.2,

$$\epsilon(p) = v_F(p - p_F)$$

The reflected hole has the momentum  $p = p_F - \epsilon/v_F$  such that  $p < p_F$ . Its energy thus corresponds to the decreasing (left) part of the spectrum branch [point (a)] in Fig. 3.2,

$$\epsilon(p) = v_F(p_F - p)$$

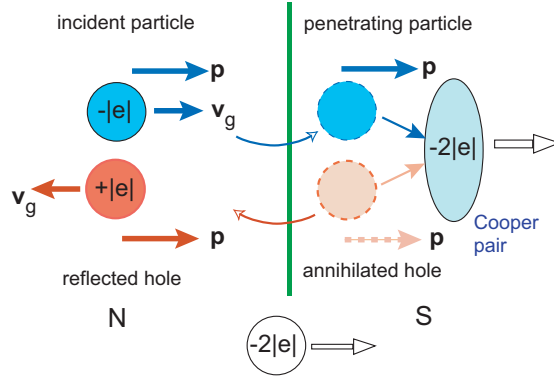


Figure 3.3: Illustration of the nature of Andreev reflection for  $\epsilon < |\Delta|$  at an ideal SN interface: An incident electron forms a Cooper pair in the superconductor together with an annihilated hole. This hole is expelled into the normal metal and moves back as a reflected object.

One can calculate the components of the group velocity

$$v_{gx} = \frac{\partial \epsilon}{\partial p_x} = \pm \frac{p_x}{m} \approx \pm v_x, \quad v_{gy} = \frac{\partial \epsilon}{\partial p_y} = \pm \frac{p_y}{m} \approx \pm v_y$$

We see that particle and hole have opposite signs of the group velocity but with almost the same magnitude. Therefore, Andreev reflected hole moves *along the same trajectory as the incident particle but in the opposite direction!*

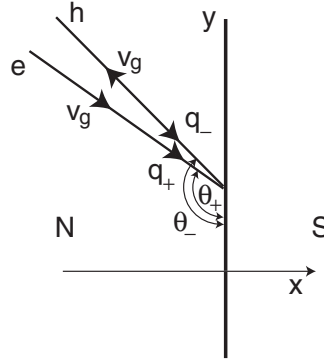


Figure 3.4: The trajectories of an incident particle and the Andreev reflected hole.

In fact, directions of the incident and reflected trajectories are slightly different. Indeed, the change in the momentum during the Andreev reflection is

$$\Delta p_x = (\hbar k_x - \epsilon/v_x) - (\hbar k_x + \epsilon/v_x) = -2\epsilon/v_x$$

This change is much smaller than the momentum itself. This is because the energy of interaction  $\sim \Delta$  is much smaller than  $E_F$ . At the same time, the momentum projections  $p_y$  and  $p_z$  are conserved. As a result, the trajectory of the reflected hole deviates, but only slightly, from the trajectory of the incident particle (see Fig. 3.4).



# Chapter 4

## Weak links

### 4.1 Josephson effect

A supercurrent can flow through a junction of two superconductors separated by narrow constriction, by a normal region or by a high-resistance insulating barrier, or by combinations of these. This is the *Josephson effect* (B. Josephson, 1962). The current is a function of the phase difference between the two superconductors. These junctions are called weak links. There may be various dependencies of the current on the phase difference. The form of this dependence and the maximum supercurrent depend on the conductance of the junction: The smaller is the conductance the closer is the dependence to a simple sinusoidal shape.

The presence of a supercurrent is a manifestation of the fundamental property of the phase coherence that exists between two superconductors separated by a weak link.

#### 4.1.1 D.C and A.C. Josephson effects

The general features of the Josephson effect can be understood using a very general example of transitions between two superconductors. Assume that two superconducting pieces are separated by a thin insulating layer. Electrons can tunnel through this barrier. Assume also that a voltage  $V$  is applied between the two superconductors.

The wave function of superconducting electrons is a sum

$$\Psi = \sum_{\alpha} C_{\alpha}(t)\psi_{\alpha}$$

of the states  $\psi_1$  and  $\psi_2$  in superconductor 1 or superconductor 2, respectively. Each wave function  $\psi_1$  and  $\psi_2$  of an uncoupled superconductor, taken separately, obeys the Schrödinger equation

$$i\hbar \frac{\partial \psi_{\alpha}}{\partial t} = E_{\alpha} \psi_{\alpha}$$

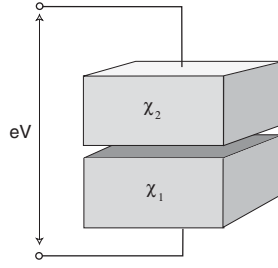


Figure 4.1: The Josephson junction of two superconductors separated by an insulating barrier.

Here  $E_\alpha$  ( $\alpha = 1, 2$ ) are the energies of the states in uncoupled superconductors 1 and 2.

When these superconductors are coupled, the wave function  $\Psi$  satisfies the Schrödinger equation

$$i\hbar \frac{\partial \Psi}{\partial t} = \hat{H} \Psi$$

where  $\hat{H}$  is the total Hamiltonian. This equation determines the variations of the coefficients. If the wave functions  $\psi_\alpha$  are normalized such that

$$\int \psi_\beta^* \psi_\alpha dV = \delta_{\alpha\beta}$$

the coefficients obey

$$i\hbar \frac{\partial C_\beta}{\partial t} = \sum_\alpha [H_{\beta\alpha} - E_\alpha \delta_{\beta\alpha}] C_\alpha(t) .$$

Here

$$H_{\beta\alpha} = \int \psi_\beta^* \hat{H} \psi_\alpha dV$$

are the matrix elements. The diagonal elements

$$H_{11} = E_1 + e^* \varphi_1 = E_1 + e^* V/2 , \quad H_{22} = E_2 + e^* \varphi_2 = E_2 - e^* V/2$$

correspond to the energies of the state 1 and 2, respectively. The charge of the Cooper pair is  $e^* = 2e$ . The off-diagonal matrix elements describe transitions between the states 1 and 2

$$H_{12} = H_{21} = -K .$$

The equation becomes

$$i\hbar \frac{\partial C_1}{\partial t} = eV C_1(t) - K C_2(t) , \quad (4.1)$$

$$i\hbar \frac{\partial C_2}{\partial t} = -K C_1(t) - eV C_2(t) . \quad (4.2)$$

The coefficients are normalized such that  $|C_1|^2 = N_1$ ,  $|C_2|^2 = N_2$  where  $N_{1,2}$  are the number of superconducting electrons in the respective electrodes. We put

$$C_1 = \sqrt{N_1}e^{i\chi_1}, \quad C_2 = \sqrt{N_2}e^{i\chi_2}.$$

Inserting this into Eqs. (4.1), (4.2) we obtain, separating the real and imaginary parts

$$\begin{aligned} \hbar \frac{dN_1}{dt} &= -2K\sqrt{N_1N_2} \sin(\chi_2 - \chi_1) \\ \hbar \frac{dN_2}{dt} &= 2K\sqrt{N_1N_2} \sin(\chi_2 - \chi_1) \end{aligned}$$

and

$$\begin{aligned} \hbar N_2 \frac{d\chi_2}{dt} &= eVN_2 + K\sqrt{N_1N_2} \cos(\chi_2 - \chi_1) \\ \hbar N_1 \frac{d\chi_1}{dt} &= -eVN_1 + K\sqrt{N_1N_2} \cos(\chi_2 - \chi_1) \end{aligned}$$

From the first two equations we obtain the charge conservation  $N_1 + N_2 = \text{const}$  together with the relation

$$I_s = I_c \sin \phi \tag{4.3}$$

where

$$I_s = 2e \frac{dN_2}{dt} = -2e \frac{dN_1}{dt}$$

is the current flowing from the first into the second electrode,  $I_c = 4eK\sqrt{N_1N_2}/\hbar$  is the critical Josephson current, while  $\phi = \chi_2 - \chi_1$  is the phase difference.

To interpret the second pair of equations we note that the overall phase of the device plays no role. Therefore we can put  $\chi_2 = \phi/2$  while  $\chi_1 = -\phi/2$ . We find after subtracting the two equations

$$\hbar \frac{\partial \phi}{\partial t} = 2eV. \tag{4.4}$$

Equation (4.3) has a familiar form and describes the so called d.c. Josephson effect: The supercurrent can flow through the insulating layer provided there is an interaction between the superconducting regions. Equation (4.4) describes the a.c. Josephson effect: the phase difference grows with time if there is a voltage between two superconductors. The d.c. and a.c. Josephson effects are manifestations of the macroscopic quantum nature of superconductivity. Various devices which employ these effects can be used for observations and for practical implementations of the quantum properties of the superconducting state.

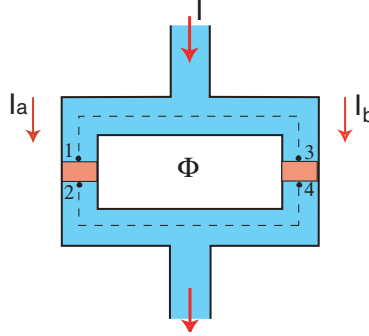


Figure 4.2: A SQUID of two Josephson junctions connected in parallel.

### 4.1.2 Superconducting Quantum Interference Devices

Equation (4.3) form a basis of SQUIDS. Consider a device consisting of two Josephson junctions in parallel connected by bulk superconductors, Fig. 4.2. Let us integrate  $\mathbf{v}_s$  defined by Eq. (1.8) along the contour that goes clockwise all the way inside the superconductors (dashed line in Fig. 4.2). We have

$$\chi_3 - \chi_1 + \chi_2 - \chi_4 - \frac{2e}{\hbar c} \left( \int_1^3 \mathbf{A} \cdot d\mathbf{l} + \int_4^2 \mathbf{A} \cdot d\mathbf{l} \right) = 0$$

since  $\mathbf{v}_s = 0$  in the bulk. Neglecting the small sections of the contour between the points 1 and 2 and between 3 and 4, we find

$$\phi_a - \phi_b = \frac{2e}{\hbar c} \oint \mathbf{A} \cdot d\mathbf{l} = \frac{2\pi\Phi}{\Phi_0} \quad (4.5)$$

where  $\phi_a = \chi_2 - \chi_1$  and  $\phi_b = \chi_4 - \chi_3$ .

The total current through the device is

$$I = I_c \sin \phi_a + I_c \sin \phi_b = 2I_c \cos \left( \frac{\pi\Phi}{\Phi_0} \right) \sin \left( \phi_a - \frac{\pi\Phi}{\Phi_0} \right).$$

The maximum current thus depends on the magnetic flux through the loop

$$I_{\max} = 2I_c \cos \left( \frac{\pi\Phi}{\Phi_0} \right). \quad (4.6)$$

Monitoring the current through the SQUID one can measure the magnetic flux.

## 4.2 Dynamics of Josephson junctions

### 4.2.1 Resistively shunted Josephson junction

Here we consider the a.c. Josephson effects in systems which carry both Josephson and normal currents in presence of a voltage. As we know, the normal current has a complicated dependence on the applied voltage which is determined

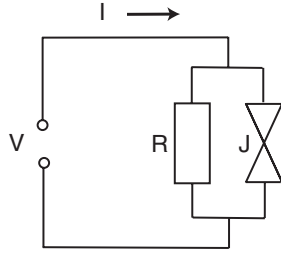


Figure 4.3: The resistively shunted Josephson junction.

by particular properties of the junction. In this Section, we consider a simple model that treats the normal current as being produced by usual Ohmic resistance subject to a voltage  $V$ . This current should be added to the supercurrent. Therefore, the total current has the form

$$I = \frac{V}{R} + I_c \sin \phi \quad (4.7)$$

where the phase difference is  $\phi = \chi_2 - \chi_1$ . Since the Josephson current through the junction is small, the current density in the bulk electrodes is also small. Thus, the phases  $\chi_1$  and  $\chi_2$  do not vary in the bulk,  $\chi_{1,2} = \text{const}$ . The difference of the phases at the both sides from the hole obeys the Josephson relation

$$\hbar \frac{\partial \phi}{\partial t} = 2eV \quad (4.8)$$

This equation describes the so called resistively shunted Josephson junction (RSJ) model (see Fig. 4.3).

The full equation for the current is

$$I = \frac{\hbar}{2eR} \frac{\partial \phi}{\partial t} + I_c \sin \phi \quad (4.9)$$

If  $I < I_c$ , the phase is stationary:

$$\phi = \arcsin(I/I_c)$$

and voltage is zero. The phase difference reaches  $\pi/2$  for  $I = I_c$ .

If  $I > I_c$ , the phase starts to grow with time, and a voltage appears. Let  $t_0$  be the time needed for the phase to grow from  $\pi/2$  to  $\pi/2 + 2\pi$ . The average voltage is then

$$(2e/\hbar)\bar{V} = 2\pi/t_0 \equiv \omega_J \quad (4.10)$$

The time  $t_0$  is found from Eq. (4.9):

$$\begin{aligned} t_0 &= \frac{\hbar}{2eR} \int_{\pi/2}^{\pi/2+2\pi} \frac{d\phi}{I - I_c \sin \phi} = \frac{\hbar}{2eR} \left( \int_{-\pi/2}^{\pi/2} \frac{d\phi}{I - I_c \sin \phi} + \int_{-\pi/2}^{\pi/2} \frac{d\phi}{I + I_c \sin \phi} \right) \\ &= \frac{I\hbar}{eR} \int_{-\pi/2}^{\pi/2} \frac{d\phi}{I^2 - I_c^2 \sin^2 \phi} = \frac{\hbar}{2eR} \frac{2\pi}{\sqrt{I^2 - I_c^2}} \end{aligned}$$

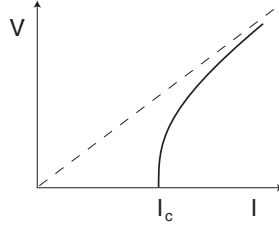


Figure 4.4: The current–voltage curve for resistively shunted Josephson junction.

The average voltage is

$$(2e/\hbar)\bar{V} = 2\pi/t_0 = \frac{2eR}{\hbar}\sqrt{I^2 - I_c^2}$$

The current–voltage curve takes the form

$$\bar{V} = R\sqrt{I^2 - I_c^2} \quad (4.11)$$

It is shown in Fig. 4.4.

### 4.2.2 The role of capacitance

The Josephson junction has also a finite capacitance. Let us discuss its effect on the dynamic properties of the junction.

The current through the capacitor (see Fig. 4.5) is

$$I = C\frac{\partial V}{\partial t}$$

The total current becomes

$$I = \frac{\hbar C}{2e}\frac{\partial^2\phi}{\partial t^2} + \frac{\hbar}{2eR}\frac{\partial\phi}{\partial t} + I_c \sin\phi \quad (4.12)$$

Let us discuss this equation. Consider first the work

$$\delta A = \int_0^{\delta t} IV dt = \frac{\hbar}{2e}I\delta\phi$$

produced by an external current source. We find

$$\delta A = \int_0^{\delta t} \frac{\partial}{\partial t} \left[ \frac{\hbar^2 C}{8e^2} \left( \frac{\partial\phi}{\partial t} \right)^2 - \frac{\hbar I_c}{2e} \cos\phi \right] dt + \frac{\hbar^2}{4e^2 R} \int_0^{\delta t} \left( \frac{\partial\phi}{\partial t} \right)^2 dt$$

This equation has the form of a balance of energy

$$\delta [E_{\text{capacitor}} + E_{\text{junction}}] = \delta A - \frac{\hbar^2}{4e^2 R} \int_0^{\delta t} \left( \frac{\partial\phi}{\partial t} \right)^2 dt$$

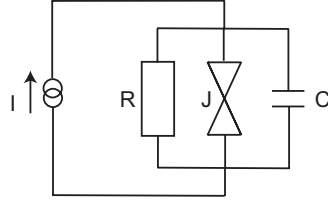


Figure 4.5: The capacitively and resistively shunted Josephson junction.

where the energy of the capacitor is

$$E_{\text{capacitor}} = \frac{\hbar^2 C}{8e^2} \left( \frac{\partial \phi}{\partial t} \right)^2 = \frac{CV^2}{2} \quad (4.13)$$

The energy of the Josephson junction is

$$E_{\text{junction}} = E_J [1 - \cos \phi], \quad \text{where } E_J = \frac{\hbar I_c}{2e} \quad (4.14)$$

The last term in the energy balance is the dissipative function.

Eq. (4.12) can also be written as a mechanical analogue equation

$$J \frac{\partial^2 \phi}{\partial t^2} + \eta \frac{\partial \phi}{\partial t} + E_J \sin \phi = F \quad (4.15)$$

of a pendulum with the moment of inertia (or “mass”)

$$J = \frac{\hbar^2 C}{4e^2} = \frac{\hbar^2}{8E_C}$$

and the maximum gravity force torque  $mgl = E_J$  in a viscous medium with a viscosity

$$\eta = \frac{\hbar^2}{4e^2 R} = \frac{\hbar^2}{8E_C R C}$$

under action of a constant torque

$$F = \frac{\hbar I}{2e}$$

Here we introduce the energy

$$E_C = \frac{e^2}{2C}$$

associated with charging the capacitor  $C$  with one electron charge. We will meet this quantity later when we discuss the Coulomb blockade effects in small junctions.

The resonance frequency of the pendulum is

$$\omega_p = \sqrt{\frac{E_J}{J}} = \sqrt{\frac{2eI_c}{\hbar C}} = \sqrt{\frac{2\pi c I_c}{\Phi_0 C}} = \frac{\sqrt{8E_J E_C}}{\hbar} \quad (4.16)$$

It is called the plasma frequency.

Equation (4.15) can be considered as an equation of motion of a particle with a coordinate  $\phi$ , a mass  $J$  in a potential

$$U(\phi) = E_J[1 - \cos \phi] - (\hbar I/2e)\phi = E_J [1 - \cos \phi - \phi I/I_c] \quad (4.17)$$

in presence of viscosity. The potential Eq. (4.17) is called a tilted washboard potential, Fig. 4.6.

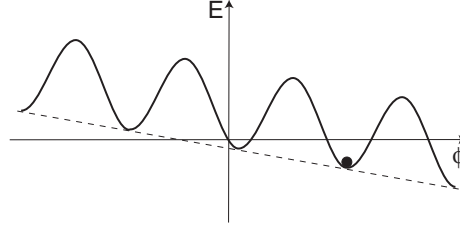


Figure 4.6: The tilted washboard potential. The tilting angle is determined by the ratio  $I/I_c$ . The dot shows a particle with a coordinate  $\phi$  in a potential minimum.

Sometimes it is convenient to introduce an effective inductance equivalent to the Josephson junction if the phase variations are small. For example, for small  $\phi$  the Josephson current becomes  $I_J = I_c \phi$ . On the other hand, due to the Josephson relation,

$$\phi = \frac{2e}{\hbar} \int V dt$$

Therefore, the Josephson current is

$$I_J = \frac{2eI_c}{\hbar} \int V dt$$

It looks like a current through an inductance where the voltage across the inductance is

$$V = \frac{1}{c} \frac{\partial \Phi}{\partial t} = \frac{L}{c^2} \frac{\partial I}{\partial t}$$

(in Gaussian units) whence

$$I = \frac{c^2}{L} \int V dt$$

Therefore, the effective inductance is

$$L_J = \frac{\hbar c^2}{2eI_c} \quad (4.18)$$

In terms of the effective inductance, the plasma frequency is

$$\omega_p = \sqrt{\frac{2eI_c}{\hbar C}} = \frac{c}{\sqrt{L_J C}}$$

which coincides with the resonance frequency of an  $LC$  circuit.

Equation (4.12) can be written also as

$$\omega_p^{-2} \frac{\partial^2 \phi}{\partial t^2} + Q^{-1} \omega_p^{-1} \frac{\partial \phi}{\partial t} + \sin \phi = \frac{I}{I_c} \quad (4.19)$$

where we introduce the quality factor

$$Q = \omega_p RC = \sqrt{\frac{2eI_c R^2 C}{\hbar}} \quad (4.20)$$

that characterizes the relative dissipation in the system. This parameter is large when resistance is large so that the normal current and dissipation are small.

Consider the dynamics of the Josephson junction in an increasing current. As long as the current is below  $I_c$ , the phase  $\phi$  is stationary: it is determined by  $I = I_c \sin \phi$ . The junction is superconducting. In the representation of a mechanical particle with a coordinate  $\phi$  in a tilted washboard potential this means that the particle is localized in one of the minima of the potential (state  $\phi_0$  in Fig. 4.7). As  $I$  increases and approaches  $I_c$ , the tilt increases, and the minima gradually disappear as shown in Fig. 4.7. For  $I > I_c$  the particle begins to roll down the potential relief. A nonzero velocity  $\partial \phi / \partial t$  determines the voltage across the junction.

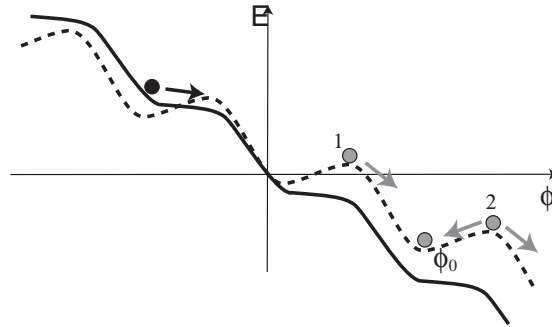


Figure 4.7: The tilted washboard potential for  $I/I_c$  close to unity. Dashed line:  $I < I_c$ , the potential has minima. Solid line:  $I > I_c$ , the minima disappear.

The current–voltage dependence is most simple for an overdamped junction which corresponds to small  $Q$  i.e., to small capacitance and large dissipation. In this case we can neglect the term with the second derivative in Eq. (4.15). We thus return to the case considered in the previous section where the current–voltage dependence is determined by Eq. (4.11).

For a finite  $Q$  the current–voltage dependence becomes hysteretic (see Fig. 4.8). With increasing current voltage is zero and the phase  $\phi$  is localized (state  $\phi_0$  in Fig. 4.7) until  $I$  reaches  $I_c$ . For  $I > I_c$  the particle rolls down the potential (solid line in Fig. 4.7), and a finite voltage appears which corresponds to a voltage jump shown by a solid line in Fig. 4.8. However, when the current

is decreased, a dissipative regime with a finite voltage extends down to currents smaller than  $I_c$ . The current at which the voltage disappears is called retrapping current. It corresponds to trapping of the particle back into one of the potential minima  $\phi_0$  in Fig. 4.7.

This behavior has a simple explanation. A particle with a small dissipation will roll down the potential overcoming the potential maxima by inertia even if  $I < I_c$  provided the loss of energy during its motion from one maximum (state 1 in Fig. 4.7) to the next (state 2) is smaller than the energy gain  $(\hbar/2e)I\delta\phi = \pi\hbar I/e$ . If the dissipation is larger (i.e.,  $Q$  is smaller), the energy loss exceeds the energy gain and the particle has no energy to continue its motion, thus it falls down into the potential minimum and remains trapped there (state  $\phi_0$  in Fig. 4.7). In a sense, this describes a transition from “insulating” to superconducting state with *increasing dissipation*.

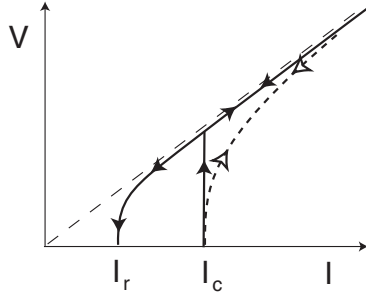


Figure 4.8: The current–voltage curve for resistively and capacitively shunted Josephson junction. The dotted line (coinciding with Fig. 4.4) is for resistively shunted junction, small  $Q$ . The solid lines show the hysteretic behavior of a contact with a large  $Q$ .

It can be shown that, for a highly underdamped junction, i.e., for large  $Q \rightarrow \infty$ , the retrapping current goes to zero while the I–V curve has the linear Ohmic dependence. For large  $Q$ , the voltage is almost constant  $V \approx \bar{V}$ , even at  $I \sim I_c$  and the phase has the form

$$\phi = 2e\bar{V}t/\hbar + \delta\phi$$

where  $\delta\phi \ll 1$ . Indeed, Eq. (4.19) yields for the time-independent component

$$\frac{2e\bar{V}}{\hbar} = \frac{Q\omega_p I}{I_c} = \frac{2eIR}{\hbar}$$

where we use Eqs. (4.16) and (4.20) so that the I–V curve is linear

$$\bar{V} = IR$$

For the oscillating component we have

$$\omega_p^{-2} \frac{\partial^2 \delta\phi}{\partial t^2} + Q^{-1} \omega_p^{-1} \frac{\partial \delta\phi}{\partial t} + \sin(\omega_J t) = 0$$

where we put

$$\omega_J = \frac{2e\bar{V}}{\hbar}$$

For a large  $Q$  we neglect the first derivative and find

$$\delta\phi = \frac{\omega_p^2}{\omega_J^2} \sin(\omega_J t)$$

The variation  $\delta\phi$  is small if  $\omega_p/\omega_J \ll 1$ . This condition reads

$$\frac{\omega_p^2}{\omega_p \omega_J} = \frac{I_c}{I \omega_p RC} = \frac{I_c}{IQ} \ll 1$$

Therefore it should be  $I_c/IQ \ll 1$ . If the current does not satisfy this condition,  $\delta\phi$  becomes large, and the finite voltage regime breaks down. Therefore, the retrapping current is

$$I_r \sim I_c/Q \quad (4.21)$$

It goes to zero as  $Q \rightarrow \infty$ .

### 4.2.3 Thermal fluctuations

Consider first overdamped junction. A particle with a coordinate  $\phi$  is mostly sitting in one of the minima of the washboard potential in Fig. 4.6. It can go into the state in a neighboring minimum if it receives the energy enough to overcome the barrier. This energy can come from the heat bath, for example, from phonons. The probability of such a process is proportional to  $\exp(-U/T)$  where  $U$  is the height of the barrier as seen from the current state of the particle. The probability  $P_+$  to jump over the barrier from the state  $\phi_0$  to the state  $\phi_0 + 2\pi$  and the probability  $P_-$  to jump over the barrier from the state  $\phi_0 + 2\pi$  back to the state  $\phi_0$  are

$$P_{\pm} = \omega_a \exp \left[ -\frac{U_0 \mp (\pi\hbar I/2e)}{T} \right]$$

where  $\omega_a$  is a constant attempt frequency, and  $U_0$  is the average barrier height. Therefore, the probability that the particle will go from the state  $\phi_0$  to the state  $\phi_0 + 2\pi$  is

$$P = P_+ - P_- = 2\omega_a \exp \left[ -\frac{U_0}{T} \right] \sinh \left( \frac{\pi\hbar I}{2eT} \right)$$

This will produce a finite voltage

$$\bar{V} = \left( \frac{\hbar}{2e} \right) 2\pi P = \frac{2\pi\hbar\omega_a}{e} \exp \left[ -\frac{U_0}{T} \right] \sinh \left( \frac{\pi\hbar I}{2eT} \right)$$

For low currents,  $I \ll I_c$ , the barrier height is independent of the current  $U_0 = 2E_J$ . For  $I \rightarrow 0$  we find

$$\bar{V} = \frac{\pi^2\hbar^2\omega_a I}{e^2 T} \exp \left( -\frac{2E_J}{T} \right)$$

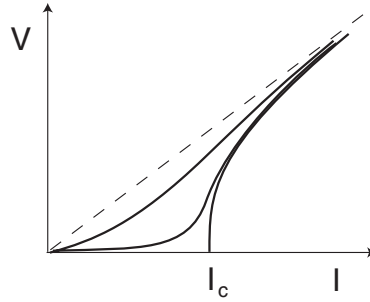


Figure 4.9: The current–voltage curves of a RSJ junction in presence of thermal fluctuations. The curves from bottom to top correspond to decreasing  $E_J/T$ ; the curve starting at  $I = I_c$  refers to  $E_J = \infty$ .

This is a linear dependence characterized by certain resistance that depends on the attempt frequency. One can express the attempt frequency in terms of the resistance in the normal state  $R$ . Indeed, for  $T^* \sim E_J$  the Josephson barrier is ineffective thus the exponent can be replaced by unity, and the current voltage dependence defines the normal resistance

$$\frac{\pi^2 \hbar^2 \omega_a}{e^2 T^*} = R$$

whence  $\omega_a = e^2 E_J R / \pi^2 \hbar^2$ . Using this we find for the voltage

$$\bar{V} = \frac{E_J R I}{T} \exp\left(-\frac{2E_J}{T}\right)$$

This determines the effective resistance of the junction [?]

$$R_J = \frac{E_J R}{T} \exp\left(-\frac{2E_J}{T}\right) \quad (4.22)$$

It is exponentially small for low temperatures.

We see that the junction has a finite (though small) resistance even for low currents. The current–voltage curve for an overdamped RSJ junction in presence of thermal fluctuations is shown in Fig. 4.9.

In the case of underdamped junctions, the particle will roll down the potential relief as soon as it gets above the potential barrier. The probability of this process is just  $P = \omega_a \exp(-U/T)$ . The attempt frequency  $\omega_a$  is now the oscillation frequency in the potential minimum determined by  $\sin \phi = I/I_c$  such that

$$\omega_a^2 = \omega_p^2 \frac{\partial^2}{\partial \phi^2} \cos \phi = \omega_p^2 \left(1 - \frac{I^2}{I_c^2}\right)^{1/2}$$

The barrier height is  $U = U_{max} - U_{min}$  where  $U_{min}$  is the value of the energy Eq. (4.17) at  $\phi = \arcsin(I/I_c)$  while  $U_{max}$  is its value at  $\phi = \pi - \arcsin(I/I_c)$ .

Therefore

$$\begin{aligned} U &= 2E_J \left[ \cos \arcsin \frac{I}{I_c} - \frac{I}{I_c} \arccos \frac{I}{I_c} \right] \\ &= 2E_J \sqrt{1 - \frac{I^2}{I_c^2}} - \frac{2IE_J}{I_c} \arccos \left( \frac{I}{I_c} \right) \end{aligned} \quad (4.23)$$

The probability is more important for large currents  $I \rightarrow I_c$  when the barrier is small,

$$U \approx \frac{4\sqrt{2}}{3} E_J (1 - I/I_c)^{3/2} \quad (4.24)$$

As the current increases from zero to  $I_c$  the probability  $P = \omega_a \exp(-U/T)$  of an escape from the potential minimum increases from exponentially small up to  $P \sim \omega_p \sim 10^{10} \text{ sec}^{-1}$ . The voltage generated by escape processes is  $V \sim (\pi\hbar/e)P$ .

The rising part of the I-V curve in Fig. 4.9 for an overdamped junction near  $I_c$  is also determined by an exponential dependence  $V = (\pi\hbar/e)P_+$  where the probability  $P_+$  contains the barrier from Eq. (4.24). Indeed, the probability of the reverse process  $P_-$  is now strongly suppressed by a considerably higher barrier seen from the next potential minimum.

#### 4.2.4 Shapiro steps

When a Josephson junction is driven by an a.c. voltage (or is subject to a microwave irradiation) with a frequency  $\omega$ , the d.c. component of supercurrent through the junction exhibits the so called Shapiro steps: jumps of the current at constant voltages satisfying  $V_n = n\hbar\omega/2e$ .

Let the voltage across the junction be

$$V = V_0 + V_1 \cos(\omega t)$$

The phase difference across the junction is then

$$\phi = \phi_0 + \omega_J t + (2eV_1/\hbar\omega) \sin(\omega t)$$

where  $\omega_J = 2eV_0/\hbar$ . The supercurrent becomes

$$I = I_c \sin \phi = I_c \sum_{k=-\infty}^{\infty} (-1)^k J_k(2eV_1/\hbar\omega) \sin(\phi_0 + \omega_J t - k\omega t)$$

where  $k$  runs over integer numbers. We use here the expansion

$$\begin{aligned} e^{iz \sin \alpha} &= J_0(z) + 2 \sum_{k=1}^{\infty} J_{2k}(z) \cos(2k\alpha) + 2i \sum_{k=0}^{\infty} J_{2k+1}(z) \sin[(2k+1)\alpha] \\ &= \sum_{k=-\infty}^{\infty} J_k(z) \cos(k\alpha) + i \sum_{k=-\infty}^{\infty} J_k(z) \sin(k\alpha) \end{aligned}$$

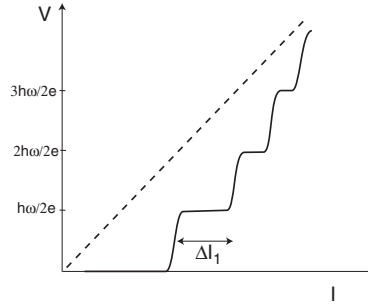


Figure 4.10: The current–voltage curves of a RSJ junction irradiated by a microwave with frequency  $\omega$ .

with  $z = 2eV_1/\hbar\omega$  and  $\alpha = \omega t$ . We note that due to the parity  $J_k(z) = (-1)^k J_{-k}(z)$  of the Bessel functions, the components with odd  $k$  drop out from the first sum in the second line, while the components with even  $k$  drop out from the second sum. Using this we arrive at the above expression for the current.

We see that for  $\omega_J = k\omega$ , i.e., for

$$V_k = k\hbar\omega/2e$$

the supercurrent has a d.c. component  $I_k = I_c J_k(2eV_1/\hbar\omega) \sin(\phi_0 + \pi k)$ . This d.c. component adds to the total d.c. current and produces the step parallel to the current axis with the width  $\Delta I_k = 2I_c J_k(2eV_1/\hbar\omega)$ .

## Chapter 5

# Coulomb blockade in normal double junctions

### 5.1 Orthodox description of the Coulomb blockade

See [12]. For more detailed description including the effects of environment see, for example, review [13], [15].

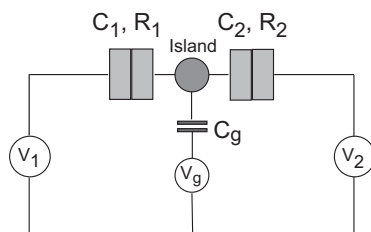


Figure 5.1: The equivalent circuit of a SET. The island is coupled to the voltage source via two contacts with resistances  $R_1$ ,  $R_2$  and capacitances  $C_1$ ,  $C_2$ , and to the gate through the capacitor  $C_g$ . The bias voltage is  $V = V_1 - V_2$ .

Consider the device called the single electron transistor (SET) with the equivalent circuit shown in Fig. 5.1. For simplicity we assume a symmetric situation  $C_1 = C_2$ ,  $R_1 = R_2 \equiv R_T$  such that  $V_1 = V/2$ ,  $V_2 = -V/2$ , and that the capacitance of the gate  $C_g$  is small. Let the charge on the island provided by the gate voltage be  $Q_0 = V_g C_g$ .

For zero bias voltage  $V = 0$ , the electrostatic energy of the island having a charge  $Q$  consisting of the continuous offset charge  $Q_0$  provided by the gate electrode and a discrete charge of  $k$  electrons that have tunneled into the island,

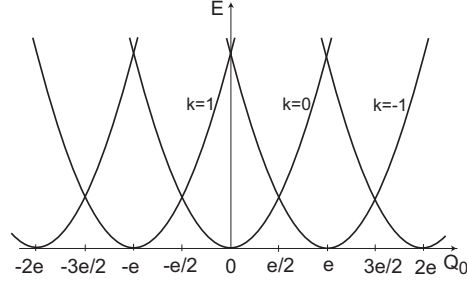


Figure 5.2:

$Q = ke + Q_0$ , is

$$\frac{Q^2}{2C_\Sigma} = \frac{(Q_0 + ke)^2}{2C_\Sigma} = \frac{Q_0^2}{2C_\Sigma} + \frac{ke(Q_0 + ke/2)}{C_\Sigma}$$

Here  $C_\Sigma = C_1 + C_2$  is the total capacitance. The spectrum is shown in Fig. 5.2. The parabolas intersect at  $Q_0 = -ke/2$ .

If the temperature is low,  $T \ll E_C$ , the tunneling into the island at small bias voltage becomes possible and the current can flow through the junction only for those gate charges for which the parabolas intersect. For other gate charges, the low-voltage current is zero. Let us consider the conditions for the current as functions of the bias voltage and the gate charge.

The energy difference between the state of the island after  $k$  electrons have tunneled from the source which has the bias potential  $V_b$  is

$$\delta E = \frac{(Q_0 + ke)^2}{2C_\Sigma} - \frac{Q_0^2}{2C_\Sigma} - keV_b = \frac{ke(Q_0 + ke/2)}{C_\Sigma} - keV_b$$

The difference vanishes when  $V_b = V_{b,k}$ , where

$$V_{b,k} = \frac{Q_0 + ke/2}{C_\Sigma}$$

For tunneling of one electron, the voltage when the tunneling starts is

$$V_{b,1} = \frac{Q_0 + e/2}{C_\Sigma}$$

[see Fig. 5.3 (a)]. It vanishes if the offset charge on the island provided by the gate is  $Q_0 = -e/2$ . For this charge, the I-V curve starts from zero voltage, Fig. 5.3 (b).

If the bias voltage is increased, the two-electron tunneling becomes possible when

$$V_{b,2} = \frac{Q_0 + e}{C_\Sigma}$$

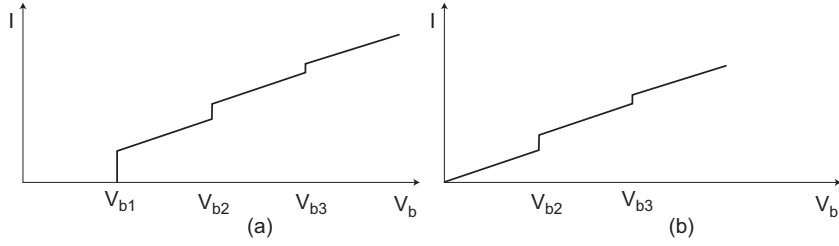


Figure 5.3: The Coulomb staircase: The current exhibits steps at  $V = V_{b,k}$ . (a) Zero offset charge  $Q_0 = 0$ , when  $V_{b,k} = (ke/2C)$ ; (b) Offset charge  $Q_0 = -e$ .

and so on. The appearance of the two-electron process is seen on the I-V curve as another step. The steps associated with multiple-charge tunneling are called the Coulomb staircase.

Let us consider now the one-electron processes and calculate the tunneling rates.

In the presence of the bias voltage, the electrostatic energy change in a state with a charge  $Q$  on the island for adding an electron to the normal island through the left junction is

$$\Delta E_L^+ = \frac{(Q+e)^2}{2C_\Sigma} - \left( \frac{Q^2}{2C_\Sigma} + \frac{eV}{2} \right) = \frac{e(Q+e/2)}{C_\Sigma} - \frac{eV}{2} = 2E_C \left( \tilde{n} + \frac{1}{2} \right) - \frac{eV}{2} \quad (5.1)$$

Here  $E_C = e^2/2C_\Sigma$  is the characteristic charging energy of the island, and  $\tilde{n} = Q/e = n + Q_0/e$  where  $n$  is an integer number of extra electrons.

In general, the electrostatic energy change in a state with a charge  $\tilde{n} = n + Q_0/e$  on the island for adding (+) or removing (-) an electron to the normal island through the left junction is

$$\Delta E_L^\pm(n) = \pm 2E_C(\tilde{n} \pm 1/2) \mp eV/2$$

The electrostatic energy change in a state with a charge  $\tilde{n}$  on the island for adding (+) or removing (-) an electron to the normal island through the right junction is

$$\Delta E_R^\pm(n) = \pm 2E_C(\tilde{n} \pm 1/2) \pm eV/2$$

The tunnelling rates are

$$\Gamma_{L(R)}^\pm(n) = \frac{1}{e^2 R_T} \int_{-\infty}^{\infty} dE f_1(E) [1 - f_2(E - \Delta E_{L(R)}^\pm(n))]. \quad (5.2)$$

Here  $R_T$  is the resistance of one contact,  $f_1(E)$  is the distributions on the source electrode, while  $f_2(E - \Delta E)$  is the distribution on the target electrode before the tunneling event; therefore  $1 - f_2(E - \Delta E)$  is the probability to find that the state is empty where the tunneling should occur. The probability of tunneling is proportional to the transparency of the contact  $\mathcal{T} \propto 1/R_T$ . The other factors

in the coefficient in front of the integral in  $\Gamma$  are chosen in such a way as to provide the correct expression for the resistance of the contact in the Ohmic regime, see Eq. (5.7) below.

For equilibrium distribution  $f_i(E) = (1 + e^{E/T_i})^{-1}$  with  $T_1 = T_2$ , we have

$$f(E)[1 - f(E - \Delta E^\pm(n))] = \frac{f(E) - f(E - \Delta E^\pm)}{1 - \exp(\Delta E^\pm/T)}$$

One can also prove that

$$\int_{-\infty}^{\infty} dE [f(E) - f(E + x)] = x$$

Therefore, Eq. (5.2) yields

$$\Gamma^\pm(n) = \frac{1}{e^2 R_T} \frac{\Delta E^\pm}{\exp(\Delta E^\pm/T) - 1} \quad (5.3)$$

The current *into* the island through the left (right) junction is

$$I_{L(R)} = e \sum_{n=-\infty}^{\infty} \sigma(n) [\Gamma_{L(R)}^+(n) - \Gamma_{L(R)}^-(n)] \quad (5.4)$$

where  $\sigma(n)$  is the probability of having  $n$  extra electrons on the island. We have

$$\sum_{n=-\infty}^{\infty} n\sigma(n) = 0 \quad (5.5)$$

by symmetry, and

$$\sum_{n=-\infty}^{\infty} \sigma(n) = 1, \quad \sum_{n=-\infty}^{\infty} \tilde{n}\sigma(n) = Q_0/e \quad (5.6)$$

### 5.1.1 Low temperature limit

For  $T \rightarrow 0$  the tunneling rates Eq. (5.3) are

$$\Gamma_{L(R)}^\pm(n) = \frac{1}{e^2 R_T} |\Delta E_{L(R)}^\pm| \Theta(-\Delta E_{L(R)}^\pm)$$

The rates vanish when all  $\Delta E_{L(R)}^\pm$  are positive. This takes place when

$$\Delta E_L^{(+)} > 0 : eV/2 - 2E_C(\tilde{n} + 1/2) < 0 \quad (a)$$

$$\Delta E_L^{(-)} > 0 : eV/2 - 2E_C(\tilde{n} - 1/2) > 0 \quad (b)$$

$$\Delta E_R^{(+)} > 0 : eV/2 + 2E_C(\tilde{n} + 1/2) > 0 \quad (c)$$

$$\Delta E_R^{(-)} > 0 : eV/2 + 2E_C(\tilde{n} - 1/2) < 0 \quad (d)$$

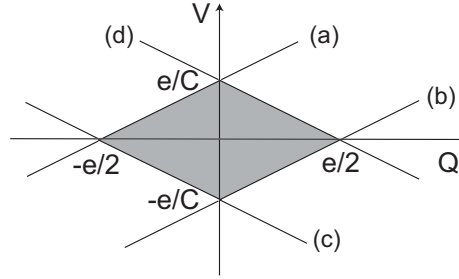


Figure 5.4: The region of stable charge is shaded. The lines (a)–(d) correspond to equalities in Eqs. (a) to (d).

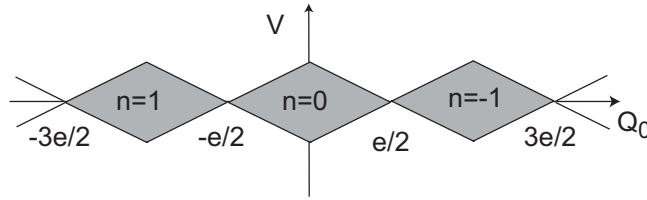


Figure 5.5: The regions of stable charge  $n = 0, \pm 1, \dots$  as functions of the gate charge.

In Fig. 5.4 the diamond-shaped region in the plane ( $V, Q = e\tilde{n}$ ) is shaded where all the rates are zero. This is the region where the current to and out of the island is zero, and the charge on the island does not change due to the Coulomb blockade. If the offset charge  $Q_0$  is in the range  $-e/2 < Q_0 < e/2$ , the state with  $n = 0$  is stable.

With change in the gate voltage, the stable charge on the island will vary by integer number of electrons due to tunneling to or from the respective electrode. The regions of stable states with  $n = 0, \pm e, \dots$  as functions of the gate charge are shown in Fig. 5.5.

### 5.1.2 Conductance in the high temperature limit

We have for the left junction

$$\Gamma_L^+(n) - \Gamma_L^-(n) = \frac{1}{e^2 R_T} \left[ \frac{\Delta E_L^+}{\exp(\Delta E_L^+/T) - 1} - \frac{\Delta E_L^-}{\exp(\Delta E_L^-/T) - 1} \right]$$

Up to the first order in  $E_C/k_B T_e$  we have

$$\begin{aligned} \Gamma_L^+(n) - \Gamma_L^-(n) &= \frac{T}{e^2 R_T} \left[ v \left( \frac{1}{1 - e^v} + \frac{1}{1 - e^{-v}} \right) \right. \\ &\quad \left. - \frac{2\tilde{n}E_C}{T} [f(v) + f(-v)] + \frac{E_C}{T} [f(v) - f(-v)] \right] \end{aligned}$$

$$= \frac{T}{e^2 R_T} \left[ v - \frac{2\tilde{n}E_C}{T} + \frac{E_C}{T} [f(v) - f(-v)] \right]$$

Here we introduce the reduced voltage  $v \equiv eV/2T$  and denote

$$f(v) = \frac{1}{1 - e^v} + \frac{ve^v}{(1 - e^v)^2}$$

We also use

$$f(v) + f(-v) = \frac{1}{1 - e^v} + \frac{1}{1 - e^{-v}} = 1$$

Using Eqs. (5.5) and (5.6) we find

$$\begin{aligned} I_L &= \frac{T}{eR_T} \left[ v - \frac{2Q_0 E_C}{eT} + \frac{E_C}{T} [f(v) - f(-v)] \right] \\ &= \frac{T}{eR_T} \left[ v - \frac{2Q_0 E_C}{eT} - \frac{E_C}{T} \frac{\sinh v - v}{2 \sinh^2 v} \right] \end{aligned}$$

We find for the differential conductance [14]

$$\frac{G}{G_T} = 2R_T \frac{dI}{dV} = 1 - \frac{E_C}{T} \frac{v \sinh v - 4 \sinh^2(v/2)}{4 \sinh^4(v/2)} \quad (5.7)$$

where  $G_T^{-1} = 2R_T$  is the total resistance of the contacts. This equation shows in particular that the resistance of the junction in the absence of charging effects is  $2R_T$ , i.e., the resistance of each tunnel contact is  $R_T$ . This confirms the choice of the coefficient in Eq. (5.2). The depth of the conductance minimum at  $V = 0$  in Eq. (5.7) is

$$\Delta G/G_T = -\frac{E_C}{3T}$$

The behavior of the conductance is shown in Fig. 5.6.

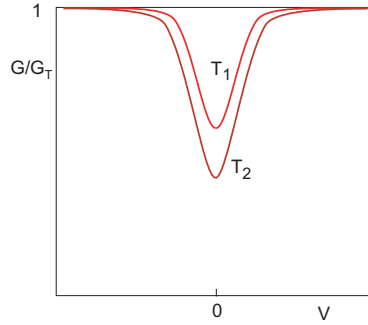


Figure 5.6: The minimum in conductance as a function of the bias voltage due to Coulomb effects at high temperatures. The two temperatures satisfy  $T_2 < T_1$ .

## Chapter 6

# Quantum phenomena in Josephson junctions

### 6.1 Quantization

#### 6.1.1 Quantum conditions

Quantum effects can be observed in Josephson structures consisting, for example, of a very small superconducting grain connected to superconducting charge reservoirs through small tunnel junctions having very low capacitance and high tunnel resistance, as shown in Fig. 6.1. The equivalent circuit is shown in Fig. 5.1. The necessary constraints can be easily estimated from general arguments. First, the Coulomb charging energy for one electron  $e^2/2C$  should be larger than temperature  $T$  to avoid thermal smearing of the charge states on the superconducting island. For  $T \sim 1$  K this gives  $C < 10^{-15}$  F which strongly restricts the size of the junction by an area  $\sim 10^{-8}$  cm<sup>2</sup>. Second, the tunnel resistance should be large enough to avoid averaging out by quantum fluctuations in the particle number. To be observable, the charging energy  $e^2/2C$  must exceed the quantum uncertainty in energy  $\hbar/\Delta t \sim \hbar/RC$  associated with the finite lifetime of the charge on the capacitor. Equating  $e^2/2C$  to  $\hbar/RC$  we find that the capacitance drops out and the condition becomes  $R > R_0$  where  $R_0$  is the resistance quantum  $R_0 = h/2e^2 \approx 12$  k $\Omega$ , the quantity already familiar from Eq. (??).

Another realization may be a small Josephson junction with a capacitance  $C$  and tunnel resistance  $R$  satisfying the above conditions, which is connected through small-capacitance,  $C_{ext} \ll C$ , high-resistance contacts such that  $R_0 \ll R_{ext} \ll R$  to the external current source, Fig. 6.2. The detailed description of quantum phenomena can be found, for example, in review [13].

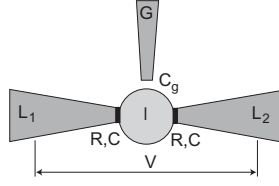


Figure 6.1: Realization of the quantum Josephson junction device: A small island  $I$  is connected to the external leads  $L_1$  and  $L_2$  by tunnel contacts. The tunnel resistance  $R$  should be larger than  $R_0$ . An additional gate electrode  $G$  is connected to the island through a capacitor  $C_g$  to control the voltage on the island.

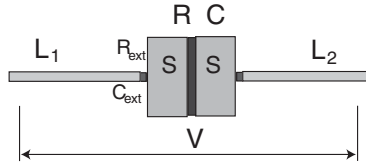


Figure 6.2: Another realization of the quantum Josephson junction device: A small Josephson junction is connected to the external leads  $L_1$  and  $L_2$  by high-resistance  $R_{ext}$  and low capacity  $C_{ext} \ll C$  contacts. Both  $R_{ext}$  and the tunnel resistance  $R$  should be larger than  $R_0$ .

### 6.1.2 Charge operator

Consider an isolated Josephson junction. The charging energy of the capacitor is

$$\frac{Q^2}{2C} = \frac{CV^2}{2} = \frac{C}{2} \left( \frac{\hbar}{2e} \frac{\partial \phi}{\partial t} \right)^2$$

If the phase difference  $\phi$  is treated as a particle coordinate, the time derivative  $\partial \phi / \partial t$  should be considered as a velocity, while the charging energy is equivalent to the kinetic energy.

In quantum mechanical description, the kinetic energy is written in terms of the momentum operator. If the coordinate is  $\phi$  then the momentum operator is defined as

$$\hat{p}_\phi = -i\hbar \frac{\partial}{\partial \phi} \quad (6.1)$$

This definition complies with the usual commutation rule

$$[\hat{p}_\phi, \phi]_- = -i\hbar \quad (6.2)$$

To find out the physical meaning of the momentum operator let us consider the continuity equation for the supercurrent

$$\frac{d(eN_s)}{dt} = - \int \frac{\partial j_{sx}}{\partial x} d^3r$$

The current density  $j$  has the form of the charge flow density  $en_s v_s$  which is

$$e \frac{\partial E_s}{\partial p_s}$$

where  $p_s$  is the momentum of a superconducting particle and  $E_s$  is the superconducting energy density. The momentum of the Cooper pair is  $2p_s = \hbar \partial \chi / \partial x$  so that the continuity equation takes the form

$$\frac{d(eN_s)}{dt} = -e \int \frac{\partial}{\partial x} \frac{\partial E_s}{\partial p_s} d^3r = -\frac{2e}{\hbar} \int \frac{\partial}{\partial x} \frac{\partial E_s}{\partial(\phi/x)} d^3r = -\frac{2e}{\hbar} \frac{\partial \mathcal{E}_s}{\partial \phi}$$

since the phase gradient over the length  $x$  is  $\partial \chi / \partial x = \phi/x$  where  $\phi$  is the (given) phase difference. The quantity

$$\mathcal{E}_s = \int E_s d^3r$$

is the superconducting energy. Therefore,

$$\frac{\hbar}{2} \frac{dN_s}{dt} = -\frac{\partial \mathcal{E}_s}{\partial \phi} \quad (6.3)$$

This equation can be considered as one of the Hamiltonian equations  $\partial p / \partial t = -\partial \mathcal{H} / \partial x$ . Since  $\phi$  is the coordinate and  $\mathcal{E}$  is the energy, the quantity  $\hbar N_s / 2$  is the momentum of the particle. However, according to Eq. (6.2) the canonically conjugated momentum operator is  $\hat{p}_\phi$ . Therefore,  $\hat{p}_\phi = \hbar N_s / 2$  and

$$-i \frac{\partial}{\partial \phi} = \frac{N_s}{2} = N_p \quad (6.4)$$

is the operator of the number of Cooper pairs  $N_p = N_s / 2$ . The second Hamiltonian equation has the form

$$\frac{\partial x}{\partial t} = \frac{\partial \mathcal{H}}{\partial p} \Rightarrow \frac{\partial \phi}{\partial t} = \frac{\mathcal{E}}{\partial(\hbar N_s / 2)} \quad \text{or} \quad \frac{1}{2} \frac{\partial \phi}{\partial t} = \frac{\partial \mathcal{E}_s}{\partial(\hbar N_s)} = \frac{\mu_s}{\hbar}$$

where  $\mu_s$  is the chemical potential of Cooper pairs. This equation coincides with the Josephson relation since  $\mu_s = eV$ .

Equation (6.4) defines the operator of “superconducting charge” transferred through the junction

$$\hat{Q} = e\hat{N}_s = 2e\hat{N}_p = -2ie \frac{\partial}{\partial \phi} \quad (6.5)$$

The commutation relation takes the form

$$[\hat{Q}, \phi]_- = -2ie$$

Therefore, the quantum uncertainty in phase  $\Delta \phi$  and in charge  $\Delta Q$  are restricted by the charge of a Cooper pair  $\Delta \phi \Delta Q \sim 2e$ .

The eigenfunction of a state with the charge  $Q$  obeys the equation

$$\hat{Q}\Psi_Q = Q\Psi_Q \quad \text{or} \quad -2ie\frac{\partial\Psi_Q}{\partial\phi} = Q\Psi_Q$$

It is

$$\Psi_Q(\phi) = Ce^{iQ\phi/2e} \quad (6.6)$$

Assuming a single-valued wave function

$$\Psi_Q(\phi + 2\pi) = \Psi_Q(\phi)$$

we obtain *quantization of charge* of a Cooper pair  $\pi Q/e = 2\pi n$ , i.e.,

$$Q = 2en$$

where  $n$  is a integer.

Note that  $\phi$  is the phase of the wave function of a Cooper *pair* of electrons. The single electron phase would be  $\phi_1 = \phi/2$ . If we now require a single-valued *one-electron* wave function,

$$\Psi_Q(\phi_1) = Ce^{iQ\phi_1/e}$$

so that  $\Psi(\phi_1 + 2\pi) = \Psi(\phi_1)$ , we obtain  $2\pi Q/e = 2\pi n$  such that the single-electron charge is integer:  $Q = en$ .

### 6.1.3 The Hamiltonian

The charging energy of a capacitor can be written as

$$\frac{Q^2}{2C} = -\frac{4e^2}{2C} \frac{\partial^2}{\partial\phi^2} = -4E_C \frac{\partial^2}{\partial\phi^2}$$

where

$$E_C = \frac{e^2}{2C}$$

is the the charging energy for the charge of one electron.

The total energy of the Josephson junction becomes

$$\mathcal{H} = -4E_C \frac{\partial^2}{\partial\phi^2} + E_J[1 - \cos\phi] \quad (6.7)$$

This is the Hamiltonian of the junction in the quantum mechanical description.

If the junction is connected to a current source, the charge operator changes

$$\hat{Q} = -2ie\frac{\partial}{\partial\phi} + q(t)$$

where  $q(t)$  is a continuous charge supplied by the current source. The Hamiltonian becomes

$$\mathcal{H} = 4E_C \left( -i\frac{\partial}{\partial\phi} + \frac{q(t)}{2e} \right)^2 + E_J[1 - \cos\phi] \quad (6.8)$$

In the classical limit this Hamiltonian is equivalent to the washboard potential. Indeed, the classical analogue of Eq. (6.8) is

$$\mathcal{E} = \frac{[Q + q(t)]^2}{2C} + E_J[1 - \cos \phi]$$

where  $Q$  is the charge that is transferred through the junction. Using the Josephson relation  $V = (\hbar/2e)(d\phi/dt)$  the charging energy can be transformed as

$$\begin{aligned} \frac{[Q + q(t)]^2}{2C} &= \frac{Q^2}{2C} + \frac{[Q + q(t)]q(t)}{C} - \frac{q^2(t)}{2C} \\ &= \frac{Q^2}{2C} + Vq(t) - \frac{q^2(t)}{2C} = \frac{Q^2}{2C} - \frac{\hbar\phi}{2e} \frac{dq}{dt} + \frac{d}{dt} \left[ \frac{\hbar\phi}{2e} q(t) \right] - \frac{q^2(t)}{2C} \\ &= \frac{Q^2}{2C} - \frac{\hbar\phi}{2e} I + \frac{dF(t)}{dt} \end{aligned}$$

Here  $I = dq/dt$ . The last term  $dF(t)/dt$  is a full derivative of certain function. It can be omitted. With Eq. (6.5) for the operator  $Q$ , the total Hamiltonian assumes the usual form of a Hamiltonian of a particle in the tilted washboard potential

$$\mathcal{H} = -4E_C \frac{\partial^2}{\partial \phi^2} + E_J[1 - \cos \phi] - \frac{\hbar I}{2e} \phi \quad (6.9)$$

The quantum-mechanical description goes over into the classical picture described in Chapter 4 when the charge  $Q$  in the charge eigen-function Eq. (6.6) is large as compared to the electron charge and can be considered as a continuous variable.

## 6.2 Macroscopic quantum tunnelling

With the account of quantum effects, the behavior of the junction in presence of a high bias current is different from that considered in the previous chapter. Consider the Hamiltonian Eq. (6.9) for a representative particle in a washboard potential. The representative particle with the coordinate  $\phi$  can now escape from the potential minimum at  $\phi_0$  by tunnelling through the potential barrier, see Fig. 6.3, maximum 1. If the maximum 2 in Fig. 6.3 is lower than the minimum  $\phi_0$ , the particle needs one tunnelling through the barrier shown by a gray region in the figure.

Tunnelling of the representative particle means a tunnelling of the entire system from one macroscopic state that contains many particles to another macroscopic state. This process involves a macroscopic number of particles and thus its probability should be inherently small. However, the Josephson junction provides a tool that can help us to observe these *macroscopic quantum tunnelling* (MQT) events.

The easiest way to solve the Schrödinger equation

$$\left[ -4E_C \frac{\partial^2}{\partial \phi^2} + U(\phi) \right] \Psi(\phi) = E\Psi(\phi)$$

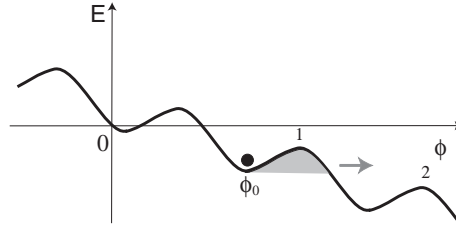


Figure 6.3: The tilted washboard potential in the quantum case. A quantum particle can escape from the potential minimum by tunnelling through the barrier (grey region).

with the washboard potential

$$U(\phi) = E_J \left[ 1 - \cos \phi - \frac{I}{I_c} \phi \right]$$

is to use the WKB approximation

$$\Psi = \exp \left( i \int \lambda(\phi) d\phi \right)$$

assuming  $d\lambda/d\phi \ll \lambda^2$ . We find

$$\lambda^2 = \frac{E - U_J(\phi)}{4E_C}$$

The WKB approximation holds if  $dU/d\phi \ll \lambda^3 E_C$  or when  $E_J \gg E_C$ .

For the energy below the potential maximum we have

$$\lambda = i\tilde{\lambda} = \frac{i\sqrt{U_J(\phi) - E}}{2E_C^{1/2}}$$

which ensures the decay of the wave function for positive  $\phi$ . The transmission probability through the barrier is proportional to the square of the transmission amplitude

$$\exp \left( - \int_{\phi_0}^{\phi'} \tilde{\lambda} d\phi \right)$$

where  $\phi_0$  and  $\phi'$  are the turning points satisfying  $E = U(\phi)$ . The probability of tunnelling becomes

$$P \sim \omega_a \exp \left( -E_C^{-1/2} \int_{\phi_0}^{\phi'} \sqrt{U_J(\phi) - E} d\phi \right) \quad (6.10)$$

The exponent is generally of the order of

$$(E_J/E_C)^{1/2} \Delta\phi \gg 1$$

where  $\Delta\phi = \phi' - \phi_0$ . This results in a very small probability. For zero current,  $\delta\phi \sim \pi$ . Writing  $\hbar\omega_p = (8E_J E_C)^{1/2}$  we can present the probability as

$$P \sim \omega_p \exp(-2\pi E_B / \hbar\omega_p)$$

where  $E_B \sim 2E_J$  is the barrier height. This will transform into the Boltzmann factor  $\exp(-E_B/T)$  for the crossover temperature

$$T_{cr} \sim \hbar\omega_p / 2\pi$$

For typical value of  $\omega_p \approx 10^{11} \text{ sec}^{-1}$  this corresponds to  $T_{cr} \approx 100 \text{ mK}$ .

The tunnelling probability increases for  $I \rightarrow I_c$ , when the barrier height is getting small, see Eq. (4.24). We have

$$U \approx \frac{4\sqrt{2}}{3} E_J (1 - I/I_c)^{3/2}$$

while

$$\Delta\phi = \arccos(I/I_c) = \sqrt{1 - (I^2/I_c^2)}$$

so that the factor in the exponent for the probability becomes

$$\sim -(E_J/E_C)^{1/2} [1 - (I/I_c)]^{5/4}$$

### 6.2.1 Effects of dissipation on MQT

For low temperatures, the system occupies the low energy states in the potential minimum with the oscillator frequency  $\omega_p$ . Consider the limit of low currents. The characteristic “time” it takes for the system to tunnel through the barrier is  $t_t \sim 2\pi/\omega_p$ . The energy dissipated during this time is

$$E_D \sim \frac{\hbar^2}{4e^2 R} \left( \frac{d\phi}{dt} \right)^2 t_t \sim \frac{2\pi\hbar^2\omega_p}{4e^2 R}$$

It should be smaller than the energy itself,  $E_D \ll \hbar\omega_p/2$ , otherwise the system cannot tunnel into a state in another potential minimum. This gives the condition

$$R \gg R_0 = \frac{h}{2e^2}$$

$R_0$  being the quantum of resistance. If this condition is fulfilled, the MQT is possible. The phase can escape from the potential minimum, and the current driven junction will exhibit a finite voltage. It will not be superconducting in a strict sense. However, if the dissipation is larger, i.e.,  $R < R_0$ , the phase cannot tunnel. There will be no voltage: the junction is superconducting. Therefore, the dissipation helps the superconductivity, which is a counterintuitive result.

We can look at this estimate also in a different way. When the phase is fixed to one of the potential minima, the charge  $Q$  on the superconducting island is not defined due to the quantum uncertainty relation. Thus, the quantum fluctuations of charge are large. On the contrary, when the phase can tunnel, its uncertainty increases and the charge becomes more localized. This agrees with the estimates on the barrier resistance made in the beginning of the present Chapter.

## 6.3 Band structure

### 6.3.1 Bloch's theorem

The Band structure of the energy states in a periodic potential is a consequence of the Bloch's theorem known in solid state physics [11]: Any solution of the Schrödinger equation for a particle in a potential  $U(x)$  periodic with a period  $a$  has the form

$$\Psi_k(x) = u_k(x)e^{ikx}$$

where  $u_k(x)$  is a periodic function

$$u_k(x+a) = u_k(x)$$

An equivalent formulation of the Bloch's theorem is that for a particle in a potential  $U(x)$  periodic with a period  $a$  there exists a quantity  $k$  such that the wave function obeys

$$\Psi_k(x+a) = e^{ika}\Psi_k(x) \quad (6.11)$$

The quantity  $k$  is called quasimomentum. The energy, i.e., the eigenvalue of the Schrödinger equation

$$\left[ -\frac{\hbar^2}{2m} \frac{d^2}{dx^2} + U(x) \right] \Psi_k(x) = E_k \Psi_k(x)$$

depends on the quasimomentum. The energy spectrum is split into intervals continuously filled by the values  $E_k$  as functions of  $k$  (energy bands) separated by intervals where there no values of  $E_k$  (forbidden bands). These energy bands are labelled by the band numbers  $n$  such that  $E = E_{kn}$ .

The quasimomentum is defined within an interval

$$-\frac{\pi}{a} \leq k \leq \frac{\pi}{a}$$

which is called the first Brillouin zone. All the quasimomenta that differ by an integer multiple of  $2\pi/a$  are equivalent, i.e., the quasimomenta

$$k' = k + (2\pi/a)n$$

refer to the same quasimomentum. Indeed, Eq. (6.11) shows that  $\Psi_{k'}(x+a) = e^{ika}\Psi_{k'}(x)$ , i.e., belongs to the same quasimomentum as  $\Psi_k$ . However, there may be *many* states belonging to the same quasimomentum, so that  $k$  and  $k + (2\pi/a)n$  do not necessarily belong to the same state. An example can be constructed for a free particle with a spectrum  $E = p^2/2m$  if one introduces a very small (zero) potential with an (arbitrary) period  $a$ . This spectrum is shown in Fig. 6.4.

Since the quasimomenta  $\pi/a$  and  $-\pi/a$  differ by  $2\pi/a$ , the points at the right and left boundary of the Brillouin zone are equivalent. One can thus consider the so called extended zone scheme where the energy is periodic as a function of quasimomentum with a period  $2\pi/a$ . This is shown in Fig. 6.4 by dashed curves.

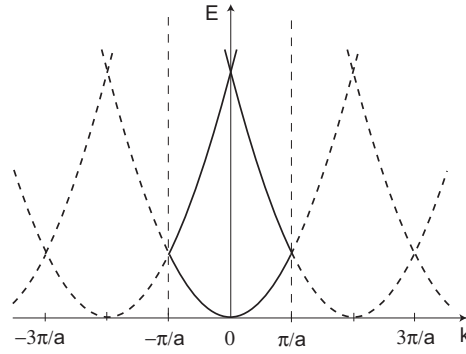


Figure 6.4: The energy spectrum for a free particle in the presence of a small periodic potential. The spectrum shown by solid lines is reduced to the first Brillouin zone  $-\pi/a < k < \pi/a$ . The dashed lines refer to the extended zone scheme.

### 6.3.2 Bloch's theorem in Josephson devices

In the case of Josephson junctions, the coordinate is  $\phi$ . If the junction is not connected to the current source, the period of the Josephson potential is  $2\pi$ . Therefore, solutions of the Schrödinger equation with the Hamiltonian Eq. (6.7)

$$-4E_C \frac{\partial^2}{\partial \phi^2} \Psi_k + E_J [1 - \cos \phi] \Psi_k = E \Psi_k \quad (6.12)$$

should obey

$$\Psi_k(\phi + 2\pi) = e^{i2\pi k} \Psi_k(\phi) \quad (6.13)$$

where  $k$  is defined within the first Brillouin zone  $-1/2 < k < 1/2$ . Equation (6.12) is known in mathematics as the Mathieu equation.

Without the potential we would have

$$\Psi_k = e^{ik\phi}$$

Comparing this with Eq. (6.6) we recognize that  $k$  plays the role of charge  $Q/2e$ . Therefore, the quasimomentum  $k$  in the presence of potential is the *quasicharge*

$$Q = 2ek$$

defined within the first Brillouin zone

$$-e < Q < e \quad (6.14)$$

If we require a single-valued wave function  $\Psi_k(\phi + 2\pi) = \Psi_k(\phi)$  we find that  $k = n$  so that the quasicharge defined within the first Brillouin zone is zero, i.e.,  $Q = 0$ . The energies of a free charge (see Fig. 6.4) are

$$E_Q = 4E_C n^2 = \frac{(2en)^2}{2C}$$

which corresponds to an integer number of electron pairs on the junction.

The situation changes if we have an external current source. The Hamiltonian has the form of Eq. (6.8). The Schrödinger equation becomes

$$4E_C \left( -i \frac{\partial}{\partial \phi} + \frac{q(t)}{2e} \right)^2 \Psi + E_J [1 - \cos \phi] \Psi = E \Psi \quad (6.15)$$

We make a gauge transformation

$$\Psi = \tilde{\Psi} e^{-iq(t)\phi/2e}$$

where the function  $\tilde{\Psi}$  satisfies Eq. (6.12) and obeys the Bloch's theorem, Eq. (6.13), i.e.,

$$\tilde{\Psi}_Q(\phi + 2\pi) = e^{i\pi Q/\epsilon} \tilde{\Psi}_Q(\phi) \quad (6.16)$$

As a result the function  $\Psi$  satisfies

$$\Psi_Q(\phi + 2\pi) = e^{i\pi[Q-q(t)]/\epsilon} \Psi_Q(\phi) \quad (6.17)$$

Requiring it to be single valued we find

$$Q = q(t) + 2en \quad (6.18)$$

whence

$$\frac{dQ}{dt} = \frac{dq}{dt} = I \quad (6.19)$$

We see that the quantum mechanics of the Josephson junction connected to the current source can be described by the Hamiltonian Eq. (6.7) where the quasimomentum depends on time according to Eq. (6.19).

### 6.3.3 Large Coulomb energy: Free-phase limit

This limit is realized when the Josephson energy  $E_J$  is much smaller than the charging energy  $E_C$ , i.e.,  $E_J \ll E_C$ . The Schrödinger equation (6.12)

$$-4E_C \frac{\partial^2}{\partial \phi^2} \Psi_Q + E_J [1 - \cos \phi] \Psi_Q = E_Q \Psi_Q \quad (6.20)$$

It has the solutions which are close to the eigenstates for fixed charge Eq. (6.6). The spectrum has the form of parabolas

$$E - E_J = E_C \frac{Q^2}{e^2} = \frac{(q + 2en)^2}{2C}$$

shown in Fig. 6.5. The parabolas are shifted by integer multiple of the Cooper pair charge  $2e$ .

The quantum-mechanical description implies that the charge  $q$  in Fig. 6.5 is replaced by a quasicharge  $Q$  reduced to the first Brillouin zone,  $-e < Q < e$ .

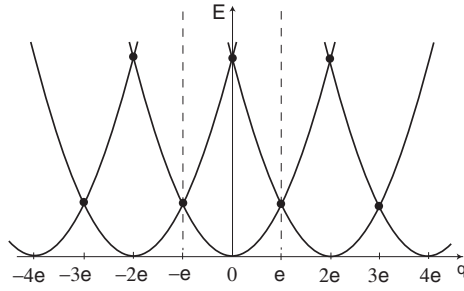


Figure 6.5: The energy spectrum of a free charge (in a zero Josephson potential) as a function of the bias charge  $q$ .

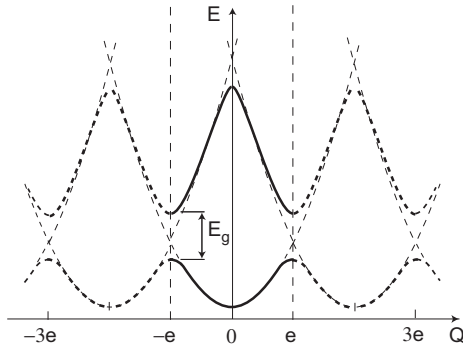


Figure 6.6: The energy spectrum for a Josephson junction in the limit of nearly free phase. The spectrum in the first Brillouin zone  $-e < Q < e$  is shown by solid lines.

A small Josephson potential introduces small energy gaps at the boundary of the Brillouin zone where the free-charge parabolas cross (black point in Fig. 6.5). To calculate the first energy gap we note that the potential

$$-E_J \cos \phi = -\frac{E_J}{2} [e^{i\phi} + e^{-i\phi}]$$

couple the states at the  $Q = e$  boundary of the Brillouin zone

$$\Psi_{Q=e} = e^{i\phi/2}$$

and the states at the  $Q = -e$  boundary

$$\Psi_{Q=-e} = e^{-i\phi/2}$$

which differ by  $\delta Q = 2e$  and thus belong to the same quasicharge  $Q$ . The wave function at  $Q = e$  will thus be a linear combination

$$\Psi_e = c_1 e^{i\phi/2} + c_2 e^{-i\phi/2}$$

Inserting this into the Schrödinger equation (6.20) we find

$$\begin{aligned} E_C \left[ c_1 e^{i\phi/2} + c_2 e^{-i\phi/2} \right] - \frac{E_J}{2} \left[ c_1 e^{3i\phi/2} + c_2 e^{i\phi/2} + c_1 e^{-i\phi/2} + c_2 e^{-3i\phi/2} \right] \\ = (E - E_J) \left[ c_1 e^{i\phi/2} + c_2 e^{-i\phi/2} \right] \end{aligned}$$

The harmonics with  $\pm 3i\phi/2$  couple to the  $Q = 3e$  quasicharge. Comparing the coefficients at the  $\pm i\phi/2$  harmonics we find

$$\begin{aligned} (E_C - E + E_J)c_1 - \frac{E_J}{2}c_2 &= 0 \\ (E_C - E + E_J)c_2 - \frac{E_J}{2}c_1 &= 0 \end{aligned}$$

whence

$$E = (E_C + E_J) \pm \frac{E_J}{2}$$

This means that the energy gap has the width  $E_g = E_J$  with the middle at  $E_C + E_J$ , see Fig. 6.6. The middle point is shifted with respect to its free-phase-limit ( $E_J = 0$ ) location at  $E_C$  due to the constant component of the potential. The lowest energy is also shifted above zero, see Problem 7.1.

Since the boundaries  $Q = -e$  and  $Q = e$  of the Brillouin zone are equivalent, as well as they are, in general, for any  $Q = 2em$  ( $m$  is an integer), one can use the so called extended zone scheme where the energy in each band  $E_{Q,n} \equiv E_n(Q)$  is a periodic function of  $Q$ :

$$E_n(Q + 2em) = E_n(Q)$$

This is shown by dashed lines in Figs. 6.4, 6.6.

### 6.3.4 Low Coulomb energy: Tight binding limit

In this limit the Josephson energy is larger than the charging energy  $E_J \gg E_C$  which implies large capacitance. The system behavior is close to that for a particle in a series of deep potential wells. One can expand the potential near each minimum

$$U(\phi) = \frac{E_J \phi^2}{2}$$

to get the oscillator potential. The Schrödinger equation (6.20) transforms into the oscillator equation

$$-4E_C \frac{d^2 \psi}{d\phi^2} + \frac{E_J \phi^2}{2} \psi = E \psi$$

The energy spectrum is

$$E_n = \sqrt{8E_C E_J} \left( n + \frac{1}{2} \right) = \hbar \omega_p \left( n + \frac{1}{2} \right)$$

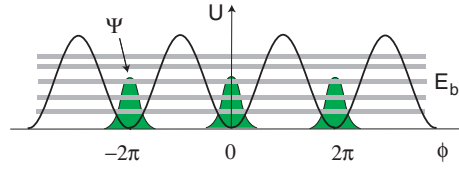


Figure 6.7: The energy band spectrum for a Josephson junction in the limit of large Josephson energy (tight binding). The energy bands are widened oscillator levels for a localized particle with the wave function  $\psi$ .

The energy spacing  $\hbar\omega_p \sim E_J \sqrt{E_C/E_J} \ll E_J$ . The lowest energy wave function is

$$\psi_0(\phi) = C \exp\left(-\frac{\phi^2}{4} \sqrt{\frac{E_J}{2E_C}}\right)$$

Due to the periodic nature of the potential one can construct the true wave function

$$\Psi_{Q,n}(\phi) = \sum_m e^{i2\pi m(Q/2e)} \Psi_n(\phi - 2\pi m)$$

where  $\Psi_n(\phi - 2\pi m)$  is a function centered at  $\phi = 2\pi m$ . The function  $\Psi_n(\phi)$  is called the Wannier function [11]. It is close to the wave function  $\psi_n(\phi)$  obtained by solving the equation near each minimum. This wave function  $\Psi_{Q,n}(\phi)$  satisfies the Bloch condition Eq. (6.16). Each level is broadened into an energy band (see Problem 7.3)

$$E_Q = E_n - \frac{1}{2} E_{b,n} \cos \frac{\pi Q}{e} \quad (6.21)$$

The band width is determined by overlaps of the wave functions  $\Psi_n(\phi)$  centered at  $\phi_m = 2\pi m$ . It is exponentially small. For example, the lowest band width is

$$E_{b,0} = 32 \left(\frac{E_J E_C}{\pi}\right)^{1/2} \left(\frac{E_J}{2E_C}\right)^{1/2} \exp\left(-\sqrt{\frac{8E_J}{E_C}}\right)$$

The quantum properties of Josephson junctions are discussed in review [?].

## 6.4 Coulomb blockade

Let us consider Fig. 6.5. If we increase, by a bias current from the external source, the charge starting from  $q = 0$  for  $n = 0$  the energy will increase until it reaches the crossing point (black dot) at  $q = e$  corresponding to the charge  $e$  on the capacitor and to the voltage  $e/C$  across the capacitor. With a further increase in  $q$  the system will go over to a state with  $n = -1$  corresponding to the parabola shifted by  $2e$  to the right that has a lower energy. The transition from  $n = 0$  to  $n = -1$  corresponds to the  $2e$  charge transfer through the

tunnel Josephson junction. We see that the charge transfer (current) through the capacitor occurs only when the voltage reaches a threshold value  $V_C = e/C$ . This is the *Coulomb blockade*: preventing of the charge transfer by the charging energy. To describe the Coulomb blockade quantum-mechanically, we need first to consider the semi-classical equation of motion in a periodic potential.

### 6.4.1 Equation of motion

In the semi-classical theory than neglects transition between energy bands, the equation of motion for the quasimomentum of a particle is [11]

$$\hbar \frac{\partial k}{\partial t} = F$$

For a constant force  $F$  this gives  $\hbar k = Ft$ . The velocity is

$$\frac{\partial x}{\partial t} = \frac{\partial E_n}{\hbar \partial k}$$

where  $E_n(k)$  is the band energy. This yields

$$\frac{\partial x}{\hbar \partial k} = \frac{1}{F} \frac{\partial E_n}{\hbar \partial k}$$

or

$$x = F^{-1} E_n(k), \quad \hbar k = Ft$$

For a free particle in zero potential  $E(k) = \hbar^2 k^2 / 2m$ , so that the particle is continuously accelerated. However, in a periodic potential,  $E(k)$  is a periodic function. Therefore, instead of being accelerated, the coordinate of particle performs *Bloch oscillations* with the amplitude  $\Delta x = 2E_b/F$  and a period

$$t = \frac{2\pi\hbar}{aF}$$

In a first Brillouin zone picture, the particle is moving until it is reflected at the zone boundary such that its quasimomentum changes from  $k_B = \pi/a$  at one boundary to  $k_B - 2\pi/a = -k_B$  at another boundary.

### 6.4.2 Bloch oscillations and the Coulomb blockade in Josephson junctions

Consider low currents such that the (Zener) transitions from one band to another have low probability. In a Josephson junction, the force equation has the form

$$\frac{\partial Q}{\partial t} = I \tag{6.22}$$

while

$$\frac{\partial \phi}{\partial t} = \frac{\partial E_{Q,n}}{\hbar \partial k} = \frac{2e}{\hbar} \frac{\partial E_{Q,n}}{\partial Q} \tag{6.23}$$

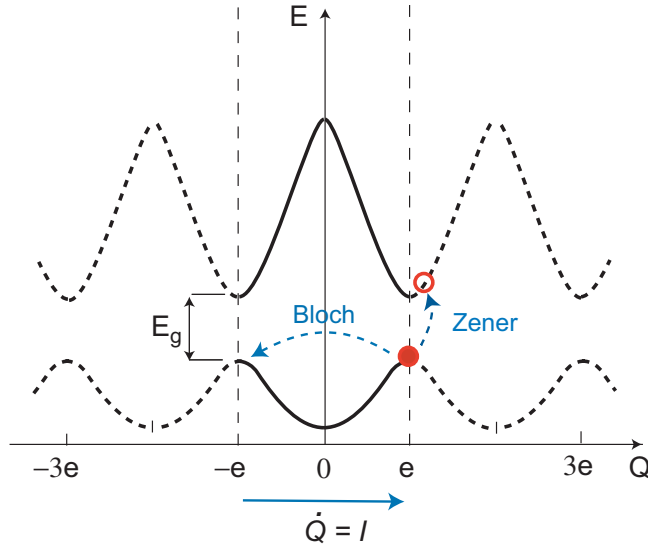


Figure 6.8: The Bloch oscillations are reflections of a particle from the Brillouin zone boundaries within one energy band. The Zener transitions between the bands lead to semiclassical behavior.

Therefore, for a constant current,

$$\frac{\partial \phi}{\partial Q} = \frac{2e}{I\hbar} \frac{\partial E_{Q,n}}{\partial Q}$$

so that

$$\phi = \frac{2e}{I\hbar} E_n(Q)$$

The period of Bloch oscillations is from Eq. (6.22)

$$t_B = \frac{2e}{I}$$

The amplitude of Bloch oscillations is

$$\Delta \phi = \frac{2e}{I\hbar} E_b$$

In the limit of large Coulomb energy (free phase),  $E_C \gg E_J$

$$E_b \approx E_C$$

and

$$\Delta \phi \approx 2eE_C/I\hbar \sim t_B/R_0C \gg 1$$

The phase is not fixed: it oscillates rapidly with a large amplitude. The voltage is

$$V = \frac{\hbar}{2e} \frac{\partial \phi}{\partial t} = \frac{\partial E_{Q,n}}{\partial Q} \approx \frac{Q}{C}$$

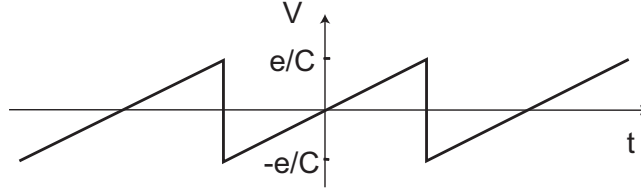


Figure 6.9: The voltage across the junction as a function of time for a constant current bias.

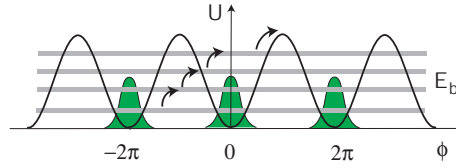


Figure 6.10: MQT is equivalent to Landau–Zener transitions between the energy bands up to the continuum. The energy bands are widened oscillator levels for a localized particle with the wave function  $\psi$ .

Each time when the quasicharge  $Q$  approaches the boundary of the Brillouin zone  $Q_B = +e$  (or  $Q_B = -e$ ), the quasicharge changes  $Q_B \rightarrow Q_B \pm 2e$  such that the voltage jumps from  $+e/C$  to  $-e/C$  (or vice versa). The average voltage is zero.

The change in the quasicharge  $Q$  by  $2e$  means the  $2e$  charge transfer through the Josephson junction. We see that the charge transfer through the junction occurs only when the voltage across the junction reaches a threshold value  $e/C$ . This is the quantum-mechanical picture of the *Coulomb blockade*. The charging energy of the junction prevents the charge transfer through it unless the voltage exceeds the threshold. At the threshold  $V_C = e/C$ , the charging energy  $Q^2/2C$  of a charge  $Q = e$  becomes equal to the charging energy  $(Q - 2e)^2/2C$  of the charge  $Q = e - 2e = -e$  on the capacitor after the Cooper pair has tunneled through the junction. To see the Coulomb blockade one needs a junction with a rather low capacity.

On the contrary, if the capacity is high such that  $E_J \gg E_C$ , the band width is very narrow, and the amplitude of phase oscillations is exponentially small. The phase is essentially fixed such that the current  $I_c \cos \phi$  flows without voltage: the junction is superconducting. A finite voltage can then appear as a result of *macroscopic quantum tunnelling* considered in the previous Section within the semiclassical approach. In the semiclassical picture of Eqs. (6.22) and (6.23), the macroscopic quantum tunnelling is equivalent to Zener transitions from a lower band up to higher bands in Fig. 6.7 and finally to the continuum for  $E > E_J$  (see Fig. 6.10). Neglecting the Zener transitions implies absence of MQT and assumes that the bias current is small.

### 6.4.3 Effect of dissipation

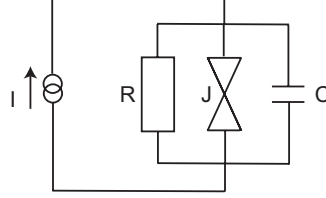


Figure 6.11: The resistively shunted Josephson junction.

Consider the resistively shunted junction, Fig. 6.11, described by [?]

$$I = \frac{\partial Q_n}{\partial t} + \frac{V}{R} \quad (6.24)$$

where, as before, the voltage across the junction

$$V = \frac{\partial E_{Q,n}}{\partial Q}$$

We again neglect the inter-band transitions assuming that the current is smaller than what is required for Zener transitions.

For high Coulomb energy,

$$\frac{\partial E_{Q,n}}{\partial Q} = \frac{Q}{C}$$

Eq. (6.24) becomes

$$\frac{\partial Q_n}{\partial t} = I - \frac{Q}{RC} \quad (6.25)$$

Assume that the charge is within the first Brillouin zone  $-e \leq Q \leq +e$ .

If the current is below the threshold value  $I < I_{th}$  where

$$I_{th} = \frac{e}{RC}$$

the current flows entirely through the shunt resistance, such that the charge and voltage are constant,  $V = Q/C = const$  and

$$I = V/R$$

If  $I > I_{th}$ , the Bloch oscillations begin. Eq. (6.25) has the solution

$$Q = Ae^{-t/RC} + IRC$$

For  $t = 0$  we have  $Q = 0$  and  $\partial Q/\partial t = I$ . This gives

$$A = -IRC$$

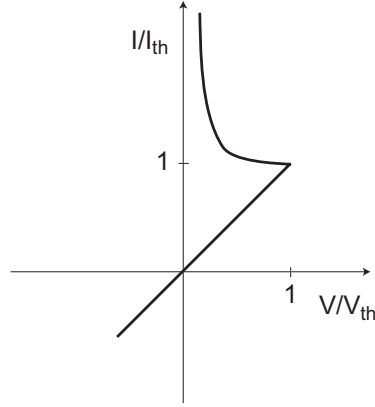


Figure 6.12: The d.c. I-V curve for resistively shunted quantum junction for the limit of high Coulomb energy.  $V_{th} = I_{th}R = e/C$ .

Assume that at  $t = -t_1$  the charge was at the end  $Q = -e$  of the Brillouin zone, while at  $t = t_2$  the charge was at the end  $Q = +e$  of the Brillouin zone. We find

$$A \exp(-t_2/RC) = e - IRC, \quad A \exp(t_1/RC) = -e - IRC$$

Therefore

$$\exp\left(\frac{t_1 + t_2}{RC}\right) = \frac{IRC + e}{IRC - e}$$

The average voltage is found from

$$\begin{aligned} (t_1 + t_2) \frac{\bar{V}}{R} &= \int_{-t_1}^{t_2} \left[ \frac{A}{RC} \exp\left(-\frac{t}{RC}\right) + I \right] dt \\ &= (t_1 + t_2) \left( I + \frac{A}{t_1 + t_2} [\exp(t_1/RC) - \exp(-t_2/RC)] \right) \end{aligned}$$

Finally,

$$\frac{\bar{V}}{R} = I - 2I_{th} \left[ \ln \frac{I + I_{th}}{I - I_{th}} \right]^{-1}$$

The second term is zero for  $I = I_{th}$  and diverges for  $I \rightarrow \infty$ . The I-V curve is shown in Fig. 6.12. The maximum d.c. voltage  $\bar{V}$  is  $V_{th} = I_{th}R = e/C$ . For  $R \rightarrow \infty$  the I-V curve is vertical which means zero d.c. voltage.

## 6.5 Parity effects

Let us consider a junction in Fig. 6.1 made of normal conductors and study how its properties change when a superconducting gap is introduced.

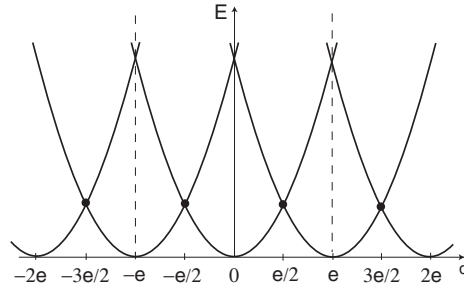


Figure 6.13: The  $e$ -periodic energy dependence of a normal junction as a function of the continuous charge  $q$  supplied by the external source.

In the case of a normal junction, the wave function depends on a single-electron phase  $\phi_1 = \phi/2$  such that the charge operator in Eq. (6.5) becomes

$$\hat{Q} = -2ie \frac{\partial}{\partial \phi} = -ie \frac{\partial}{\partial \phi_1} \quad (6.26)$$

The eigenfunction has the form

$$\Psi_Q = e^{iQ\phi_1/e}$$

which is  $2\pi$ -periodic for  $Q = ne$ . The Josephson current disappears, and the Hamiltonian becomes

$$\mathcal{H} = -E_C \frac{\partial^2}{\partial \phi_1^2}$$

If the junction is connected to the external leads, the Hamiltonian takes the form

$$\mathcal{H} = E_C \left( -i \frac{\partial}{\partial \phi_1} + \frac{q(t)}{e} \right)^2$$

The solution of the corresponding Schrödinger equation has the form

$$\Psi = e^{i(Q-q)\phi_1/e}$$

The condition of  $2\pi$ -periodicity gives  $Q = q + me$  where  $m$  is an integer.

The energy is

$$E_Q = E_C \frac{Q^2}{e^2} = E_C \frac{(q + me)^2}{e^2}$$

It is shown in Fig. 6.13. The different parabolas correspond to different values of  $m$ .

Assume we start with  $m = 0$ . As we increase the charge  $q$  supplied by the external source, the energy grows until  $q$  reaches  $e/2$  which corresponds to the voltage  $V_C = e/2C$ . At this moment, the energy of the capacitor becomes equal to the energy for the state with  $m = -1$ , i.e., to  $(q - e)^2/2C$ . At this point the charge at the capacitor decreases by  $e$ , one electron being transferred through

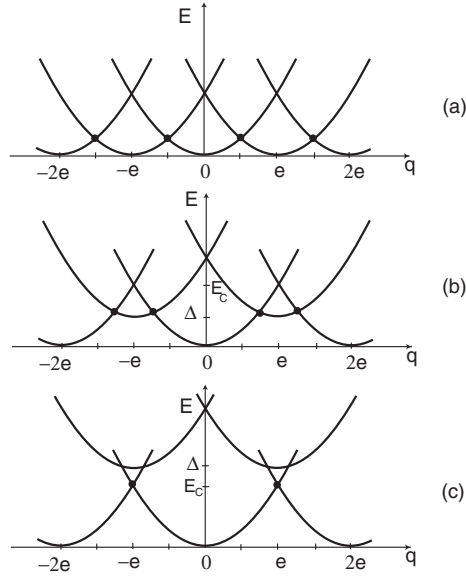


Figure 6.14: The energy of junctions. (a)  $e$ -periodic dependence in the normal state. (b) Energy of odd-number states is shifted by  $\Delta < E_C$ . The charge transfer occurs at the crossing points (black dots). (c)  $\Delta > E_C$ , the charge transfer occurs with a  $2e$  periodicity.

the junction via tunnelling. We see again that the charge transfer (current) does not occur unless voltage reaches the threshold value  $V_C$  (Coulomb blockade).

Consider again the device shown in Fig. 6.1 and apply a gate voltage  $V_G$  between the island and the gate electrode. If  $V_G = V_C$ , the energy of the junction corresponds to the level where the parabolas cross (black dots in Fig. 6.13). This means that an infinitely small voltage  $V$  can lead to a continuous transfer of charge from lead  $L_1$  to lead  $L_2$ .

Let us now assume that the island  $I$  is superconducting with an energy gap  $\Delta$ . For simplicity we restrict ourselves to zero temperatures. If the number of electrons on it is even, they all are included into Cooper pairs and form the ground state with zero energy plus the charging energy. If now we add an extra (odd) particle, it can only occupy a state above the gap thus the energy will be  $\Delta$  plus the charging energy. One more particle will make a pair with the previous one thus decreasing the total energy down to simply the charging energy. Therefore, the states with odd number of particles will have energy which is the charging energy for the given number of particles shifted by  $+\Delta$  with respect to the energy for the even number of particles. This is shown in Fig. 6.14.

Shift of the parabolas for odd particle numbers destroys the  $e$ -periodicity of the energy spectrum. When  $\Delta$  becomes larger than the charging energy  $\Delta > E_C$ , the charge transfer occurs only within the states with even number of

particles, and the  $2e$ -periodicity characteristic for a superconducting system is restored (Fig. 6.14(c)).

When also the leads become superconducting, the Josephson energy appears, and the gaps open at the crossing points shown by black dots. The energy dependence returns to Fig. 6.6 for a superconducting Josephson junction considered before.



# Bibliography

- [1] P.G. de Gennes *Superconductivity of Metals and Alloys* (W.A. Benjamin, Inc, 1965).
- [2] M. Tinkham, *Introduction to superconductivity* (McGraw-Hill, New York, 1996).
- [3] J. Bardeen, L.N. Cooper, and J.R. Schrieffer, *Phys. Rev.* **108**, 1175 (1957).
- [4] L.D. Landau and E.M. Lifshitz, *Statistical Physics Part 2: Theory of the condensed state*, by E.M. Lifshitz and L.P. Pitaevskii (Pergamon, Oxford 1980), Chapter III.
- [5] Abrikosov, A. A. *Fundamentals of The Theory of Metals*. (North Holland, Amsterdam, 1998).
- [6] D. Saint-James, G. Sarma, and E.J. Thomas *Type II superconductivity* (Pergamon Press, 1969).
- [7] R. Feynman, in: *Progress in Low Temperature Physics* vol. 1, edited by C. J. Gorter (North Holland, Amsterdam, 1955) p. 36.
- [8] A.A. Abrikosov, *Zh. Eksp. Teor. Fiz.* **32**, 1442 (1957) [*Sov. Phys. JETP* **5**, 1174 (1957)].
- [9] A. F. Andreev, *Zh. Eksp. Teor. Fiz.* **49**, 655 (1965) [*Sov. Phys. JETP* **22**, 455 (1966)].
- [10] G.E. Blonder, M. Tinkham, and T.M. Klapwijk, *Phys. Rev. B*, **25**, 4515 (1982).
- [11] J.M. Ziman, *Principles of the theory of solids*, (Cambridge University Press, 1965).
- [12] D.V. Averin and K.K. Likharev, “Single Electronics: Correlated Transfer of Single Electrons and Cooper Pairs in Systems of Small Tunnel Junctions”, in: *Mesoscopic Phenomena in Solids*, B.I. Altshuler, P.A. Lee, and R.A. Webb, eds. (Elsevier, New York 1991), p. 169.

- [13] G.-L. Ingold and Yu. V. Nazarov, “Charge tunneling rates in ultrasmall junctions”, in: *Single Charge Tunneling*, H. Grabert and M.H. Devoret, eds., NATO ASI Series, Vol. 294, pp. 21–107 (Plenum Press, New York, 1992); arXiv:cond-mat/0508728v1
- [14] J.P. Pekola, K.P. Hirvi, J.P. Kauppinen, and M.A. Paalanen, *Phys. Rev. Lett.* **94**, 2903 (1994).
- [15] Yu. V. Nazarov and Ya. M. Blanter, *Quantum Transport* (Cambridge University Press, 2009).